Supplementary Information

Application of orthogonal metal-ligand interactions for the synthesis of interpenetrating metallopolymer networks featuring shape-memory and self-healing abilities

Josefine Meurer, [a,b] Thomas Bätz, [a,b] Julian Hniopek, [c,d,e] Carolin Bernt, [a,b] Stefan Zechel, [a,b] Michael Schmitt, [c,d] Jürgen Popp, [c,d,e] Martin D. Hager [a,b] and Ulrich S. Schubert *[a,b,d]

(a) Laboratory of Organic and Macromolecular Chemistry (IOMC), Friedrich Schiller University Jena, Humboldtstr. 10, 07743 Jena, Germany, E-mail: ulrich.schubert@uni-jena.de

(b) Jena Center of Soft Matter (JCSM), Friedrich Schiller University Jena, Philosophenweg 7, 07743 Jena, Germany

(c) Institute of Physical Chemistry (IPC), Friedrich Schiller University Jena, Helmholtzweg 4, 07743 Jena, Germany

(d) Abbe Center of Photonics (ACP), Friedrich Schiller University Jena, Albert-Einstein-Straße 6, 07745 Jena, Germany

(e) Leibniz Institute of Photonic Technology, e. V. Jena, Albert-Einstein-Straße 9, 07745 Jena, Germany

Inhaltsverzeichnis

Synthesis of the linear polymers

The linear polymers **P1** and **P2** were synthesized *via* RAFT polymerization. All RAFT polymerizations were performed according to literature procedure under use of a standard approach usually applied in our group.[1-3] The polymerizations were carried out in a 250 mL one-neck-round bottom flask. The main monomer *n*-butyl methacrylate (BMA), the initiator 2,2'-azo*bis*(2-methylpropionitrile) (AIBN), 2-cyano-2-propyl dodecyl trithiocarbonate (CPDT, for synthesis of **P1**) or 2-cyano-2-propyl benzodithioate (CPDB, for the synthesis of **P2**) as chain transfer agent as well as the respective ligand monomers, N^{α}-methacryloyl-N^{τ}-tritylhistidine butyl amide (**His-MA**, for **P1**) or 6-(2,2':6'2''-terpyridin-4'-yloxy)-hexyl methacrylate (**Tpy-MA**, for **P2**), were added into the flask. Afterwards, the required amount of *N,N*-dimethyl formamide (DMF) was added until the desired concentration of 2 mol L^{-1} was reached. The [Monomer] to [CTA] ratio was 125 to 1, the ratio of [CTA] to [Initiator] 4 to 1. The utilized quantities are listed in **Table S1**. The solution was purged with nitrogen for 1 h. Afterwards, the mixture was stirred for 17 h in a preheated oil bath at 70 °C. The crude product was purified by dialysis (MWCO: 3500 g/mol, THF). The solvent was changed two times each day for three days. A summary of the determined properties via SEC, ^{1}H NMR, DSC and TGA is given in **Table S2**. The ^{1}H NMR spectra of the polymers **P1** and **P2** are displayed in **Figure S1** and **S2**.

Table S1. Utilized quantities of all substances for the synthesis of **P1** and **P2**.

	BMA	**Ligand monomer**	**AIBN**	**CTA**	**DMF [mL]**
P1	20 g 140.65 mmol	7.3 g 14.06 mmol	51 mg 0.31 mmol	428 mg 1.24 mmol	77
P2		2.9 g 7.03 mmol	49 mg 0.30 mmol	261 mg 1.18 mmol	74

P1: Anal. calcd: C 69.51, H 9.25, N 2.44; found: C 69.06, H 9.22, N 2.41.

P2: Anal. calcd: C 68.11, H 9.51, N 1.23; found: C 67.91, H 9.62, N 1.18.

Table S2: Summary of the determined molar masses and dispersities *via* SEC, calculated composition *via* ^{1}H NMR spectroscopy and thermal properties (determined glass transition temperature *via* differential scanning calorimetry (DSC) and degradation temperature *via* thermo gravimetric analysis (TGA)).

	SEC results[a]			**Monomer ratio BMA : Ligand monomer**		**Thermal properties**	
	M_n [g mol^{-1}]	**M_w [g mol^{-1}]**	**Đ**	**Utilized for synthesis**	**Calculated *via* ^{1}H NMR [b]**	**T_g [c] [°C]**	**T_d [d] [°C]**
P1	14 800	18 400	1.24	10.0 : 1	12.5 : 1	22	198
P2	10 600	12 900	1.22	20.0 : 1	20.8 : 1	10	271

[a] Eluent: $CHCl_3$/*i*-PrOH/NEt_3 (94/2/4); PMMA standard; [b] 300 MHz, CD_2Cl_2; [c] 2nd heating cycle, heating rate: 20 K min^{-1}; [d] heating rate: 10 K min^{-1}.

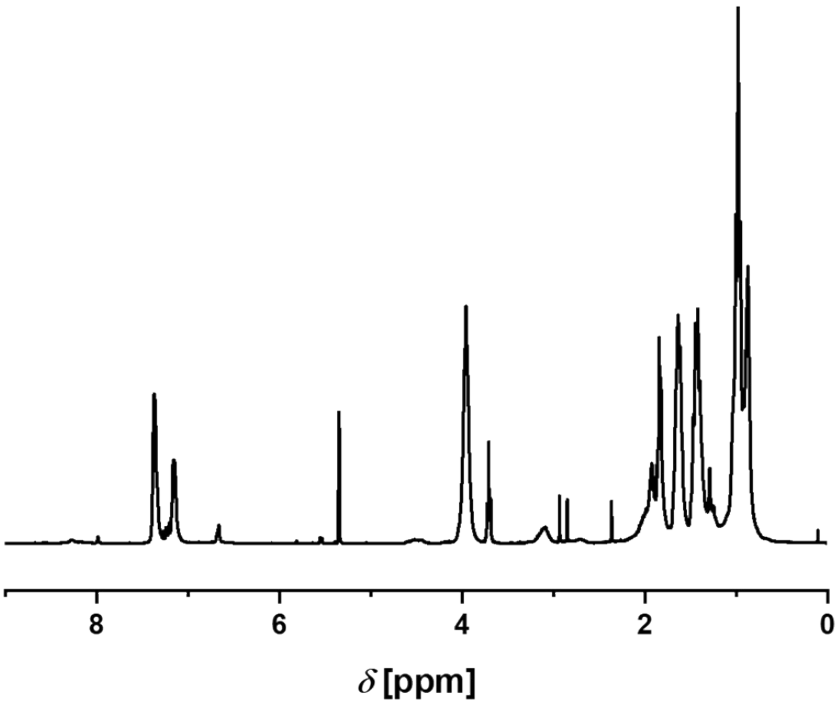

Figure S1. ^{1}H NMR spectrum of the polymer **P1** (300 MHz, CD_2Cl_2).

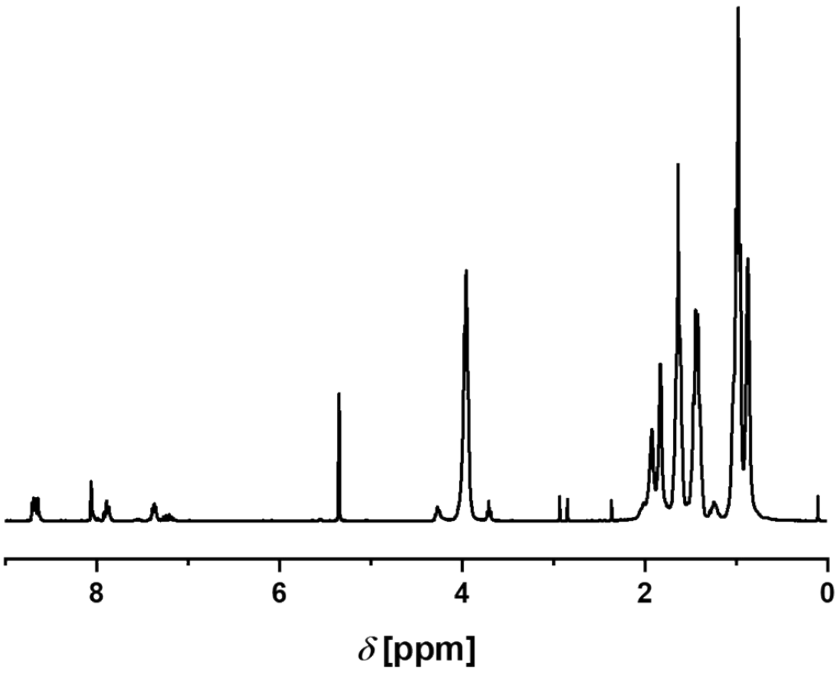

Figure S2. ^{1}H NMR spectrum of the polymer **P2** (300 MHz, CD_2Cl_2).

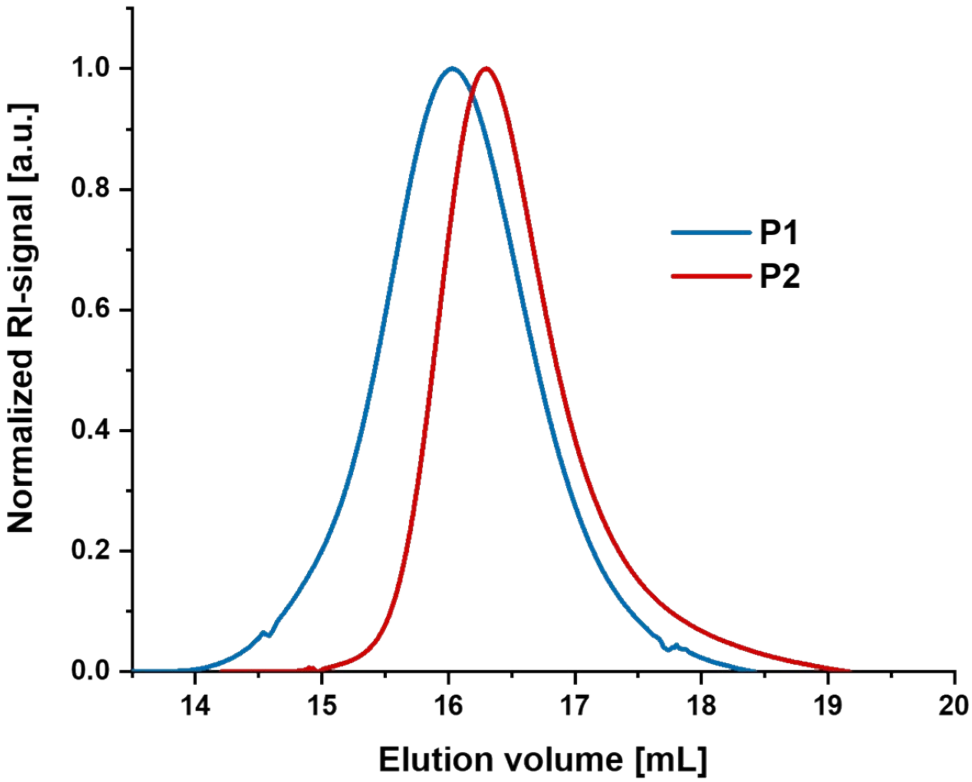

Figure S3. SEC curves of the polymers **P1** (blue) and **P2** (red) (eluent: Chloroform/*iso*-propanol/triethylamine [94/2/4]).

Synthesis of the interpenetrating metallopolymer networks

For the synthesis of the interpenetrating networks **IPN-1** to **IPN-7** a mixture of **P1** and **P2** was added into a 50 mL one-neck-round-bottom flask and dissolved in chloroform (10 mL). Subsequently, the salt or salt combination was dissolved separately in methanol and afterwards added to the dissolved polymer mixture. The solvent was removed under *vacuo* and the resulting interpenetrating metallopolymer networks were dried at a pressure of about 8 mbar overnight. The utilized quantities for each synthesis are listed in **Table S3**.

Table S3. Utilized quantities of all substances for the synthesis of **IPN-1** to **IPN-7**.

	Polym. (P)	m (P) [g]	n (P)[a] [mmol]	Salt(s) for complexation	Molar ratio	m (salt) [g]	n (salt) [mmol]
IPN-1	**P1**	2.010	0.874	$Zn(TFMS)_2$	2 : 1	160	0.437
	P2	1.013	0.298		2 : 1	54	0.149
IPN-2	**P1**	2.013	0.876	$FeSO_4 \times 7\ H_2O$	3 : 1	81	0.292
	P2	1.004	0.294		2 : 1	41	0.147
IPN-3	**P1**	2.001	0.870	$NiCl_2 \times 5\ H_2O$	3 : 1	69	0.290
	P2	1.002	0.294	$FeSO_4 \times 7\ H_2O$	2 : 1	41	0.147
IPN-4	**P1**	2.010	0.874	$Zn(TFMS)_2$	2 : 1	160	0.437
	P2	1.004	0.294	$NiCl_2 \times 5\ H_2O$	2 : 1	35	0.147
IPN-5	**P1**	2.000	0.870	$Zn(TFMS)_2$	2 : 1	159	0.435
	P2	1.000	0.294	$FeSO_4 \times 7\ H_2O$	2 : 1	41	0.147
IPN-6	**P1**	1.507	0.656	$Zn(TFMS)_2$	2 : 1	120	0.328
	P2	1.505	0.442	$FeSO_4 \times 7\ H_2O$	2 : 1	61	0.221
IPN-7	**P1**	0.756	0.328	$Zn(TFMS)_2$	2 : 1	60	0.164
	P2	1.510	0.444	$FeSO_4 \times 7\ H_2O$	2 : 1	62	0.222

[a] Based on the molar mass calculated from an artificial unit containing one ligand-entity and n x BMA repeating units (ratio of BMA and ligand unit obtained from ^{1}H NMR spectrum).

IPN-1: Anal. calcd: C 63.61, H 8.58, N 1.77, S 2.02; found: C 63.73, H 8.62, N 2.01, S 1.33.

IPN-2: Anal. calcd: C 66.09, H 9.18, N 1.95, S 0.82; found: C 65.71, H 9.09, N 2.09, S 0.68.

IPN-3: Anal. calcd: C 66.77, H 9.22, N 1.97, S 0.28; found: C 65.65, H 9.04, N 2.06, S 0.39.

IPN-4: Anal. calcd: C 64.52, H 8.80, N 1.80, S 1.37; found: C 64.67, H 8.87, N 2.07, S 1.05.

IPN-5: Anal. calcd: C 64.11, H 8.77, N 1.78, S 1.70; found: C 64.90, H 8.89, N 2.06, S 1.15.

IPN-6: Anal. calcd: C 64.42, H 8.94, N 1.61, S 1.44; found: C 65.25, H 8.82, N 1.95, S 1.08.

IPN-7: Anal. calcd: C 64.69, H 9.08, N 1.45, S 1.22; found: C 65.59, H 8.93, N 1.77, S 0.92.

Synthesis of model metallopolymer networks

For comparison of the results from the Raman-spectroscopic investigations, several model metallopolymers, containing only one polymer and one salt, were synthesized. For the synthesis, the polymer **P1** or **P2** was added into a 10 mL flask and dissolved in chloroform (3 mL). Subsequently, the salt was separately dissolved in methanol (1 mL) and afterwards added to the dissolved polymer. The solvent was removed under *vacuo* and the resulting metallopolymer network was dried at a pressure of about 8 mbar overnight. The utilized quantities are listed in **Table S4**.

Table S4. Utilized quantities of all substances for the synthesis of the model polymer networks (**P1-Fe**, **P1-Ni**, **P1-Zn**, **P2-Fe**, **P2-Ni** and **P2-Zn**).

	Polymer (P)	m (P) [mg]	n (P) [a] [mg]	Salt for complexation	Molar ratio	m (salt) [mg]	n (salt) [mmol]
P1-Fe	**P1**	191	0.087	$FeSO_4 \times 7\ H_2O$	3 : 1	8	0.028
P1-Ni		202	0.084	$NiCl_2 \times 5\ H_2O$	3 : 1	7	0.029
P1-Zn		215	0.094	$Zn(TFMS)_2$	2 : 1	17	0.047
P2-Fe	**P2**	198	0.058	$FeSO_4 \times 7\ H_2O$	2 : 1	8	0.029
P2-Ni		207	0.060	$NiCl_2 \times 5\ H_2O$	2 : 1	7	0.030
P2-Zn		195	0.058	$Zn(TFMS)_2$	2 : 1	10	0.029

[a] Based on the molar mass calculated from an artificial unit containing one ligand-entity and n x BMA repeating units (ratio of BMA and ligand unit obtained from ^{1}H NMR spectrum).

Thermo gravimetric analyses (TGA)

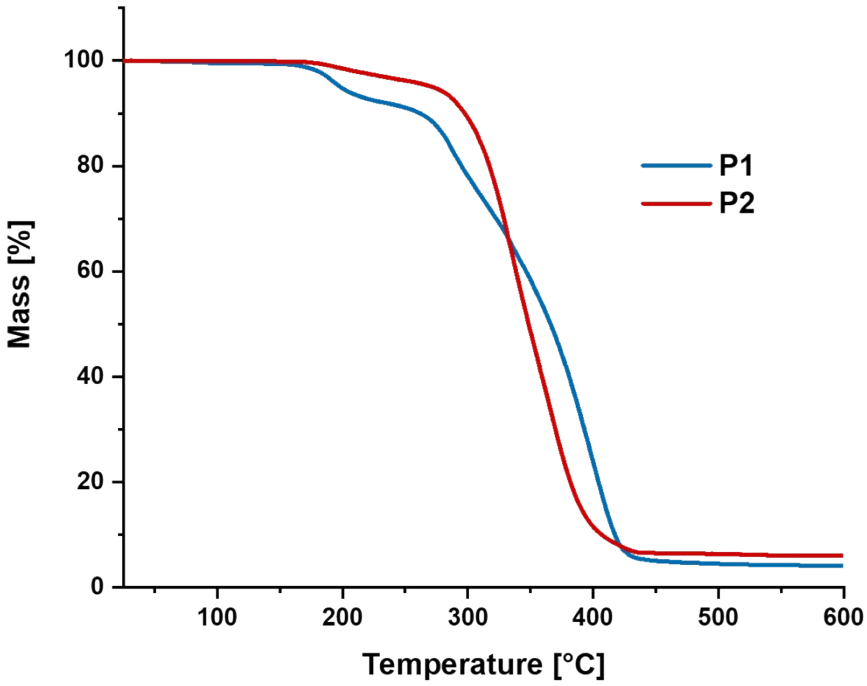

Figure S4. TGA-curves of the polymers **P1** (blue) and **P2** (red).

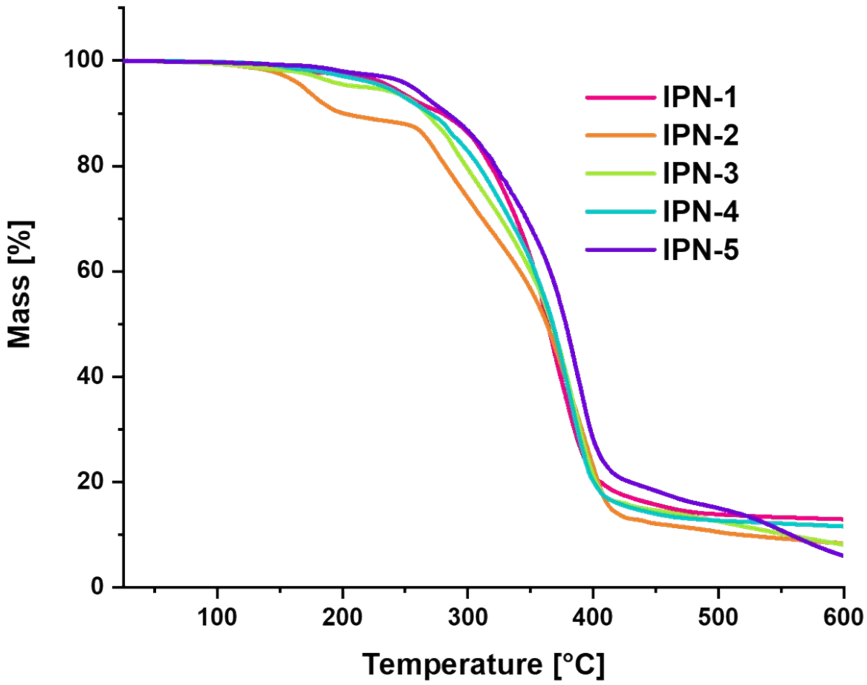

Figure S5. TGA-curves of **IPN-1** (pink), **IPN-2** (orange), **IPN-3** (green), **IPN-4** (turquoise) and **IPN-5** (blue).

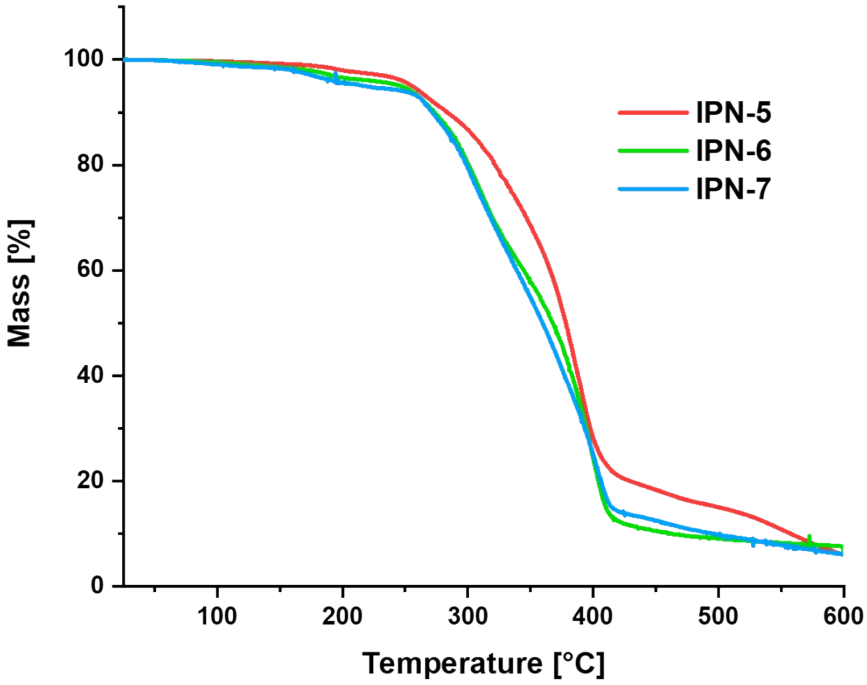

Figure S6. TGA-curves of **IPN-5** (red), **IPN-6** (green) and **IPN-7** (blue).

Differential scanning calorimetry (DSC)

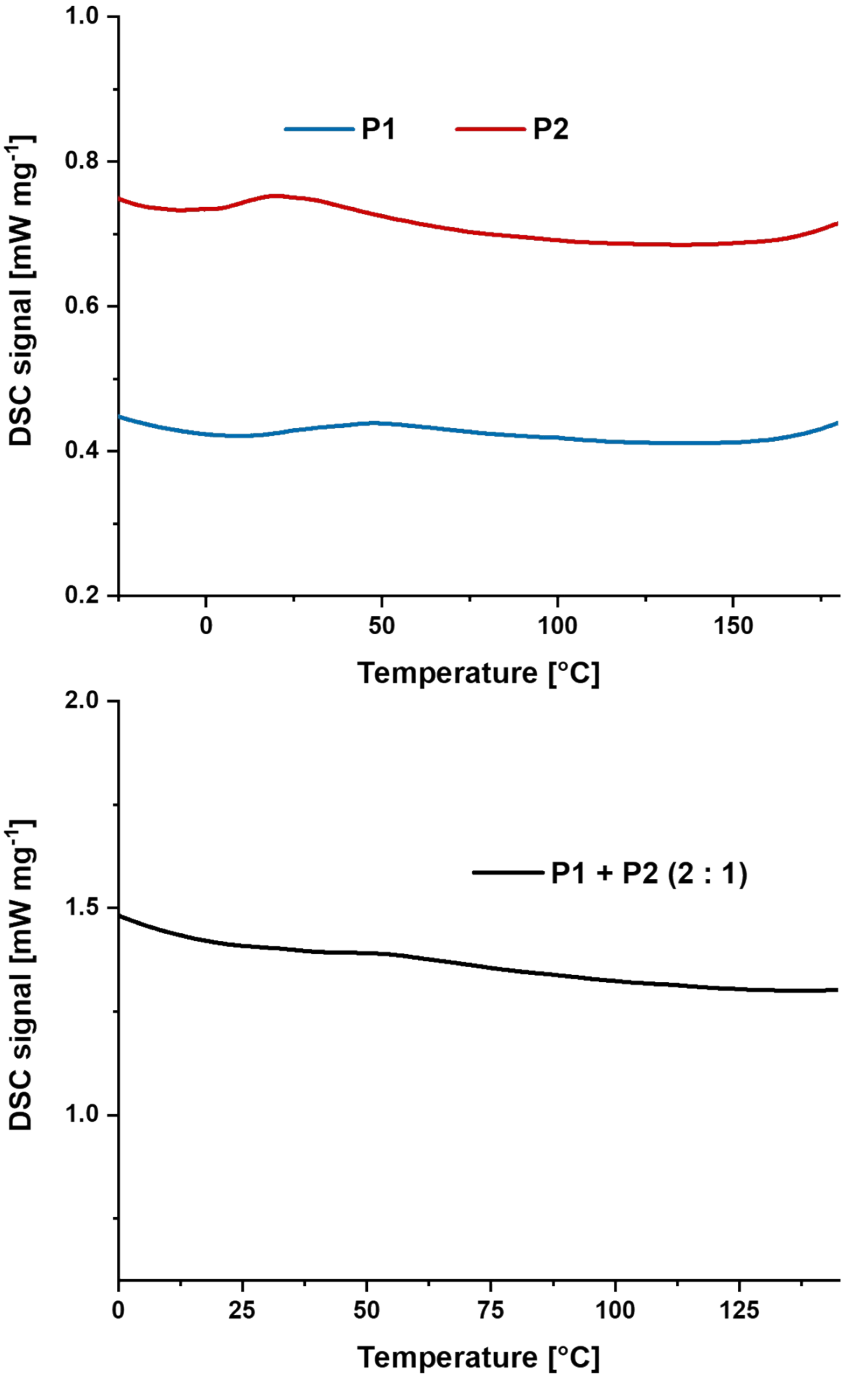

Figure S7. DSC-curves of the second heating cycle of top: the single polymers **P1** (blue) and **P2** (red) and bottom: the mixture of **P1** and **P2** (2 :1).

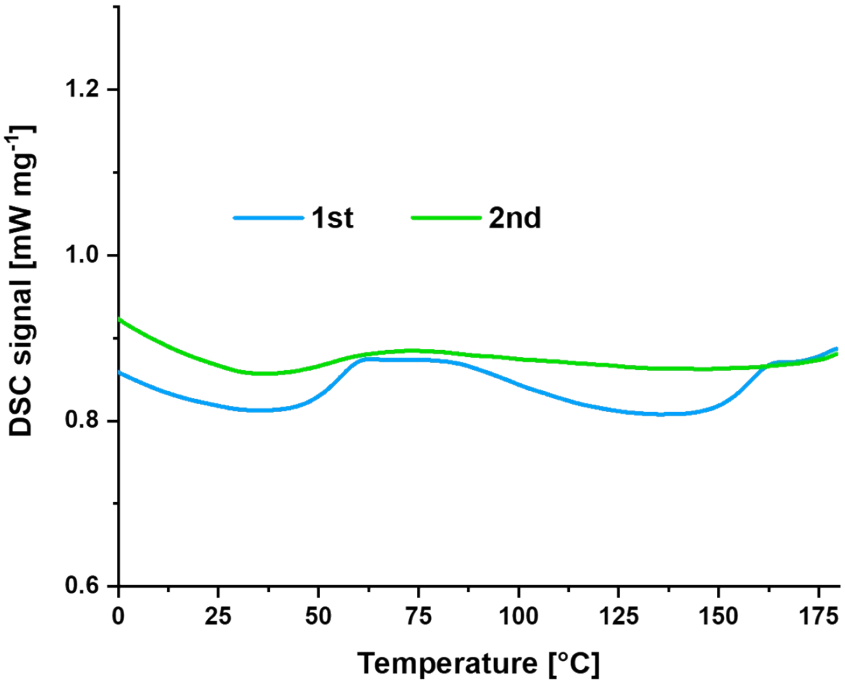

Figure S8. DSC-curves of the first (blue) and second (green) heating cycle of **IPN-1**.

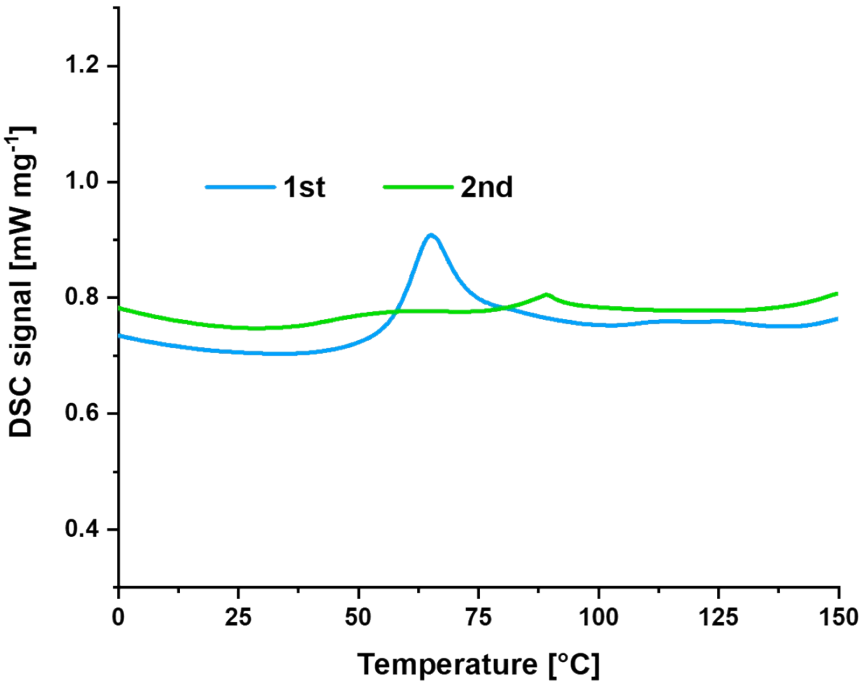

Figure S9. DSC-curves of the first (blue) and second (green) heating cycle of **IPN-2**.

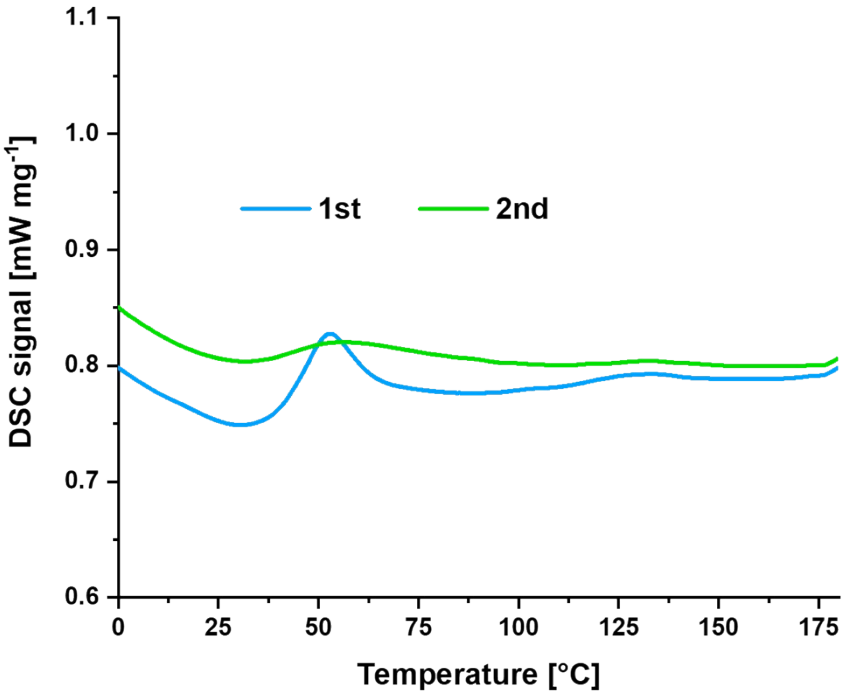

Figure S10. DSC-curves of the first (blue) and second (green) heating cycle of **IPN-3**.

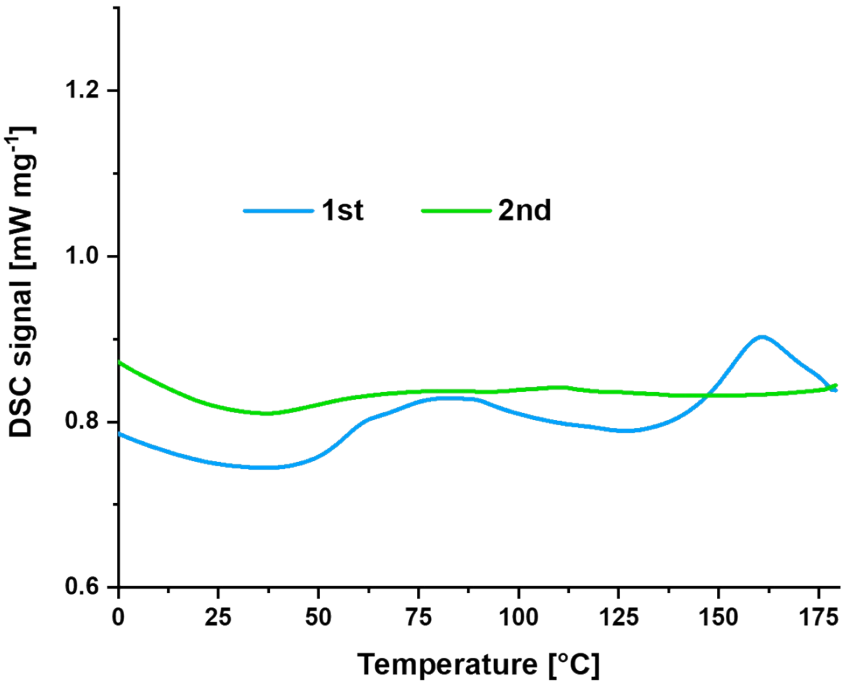

Figure S11. DSC-curves of the first (blue) and second (green) heating cycle of **IPN-4**.

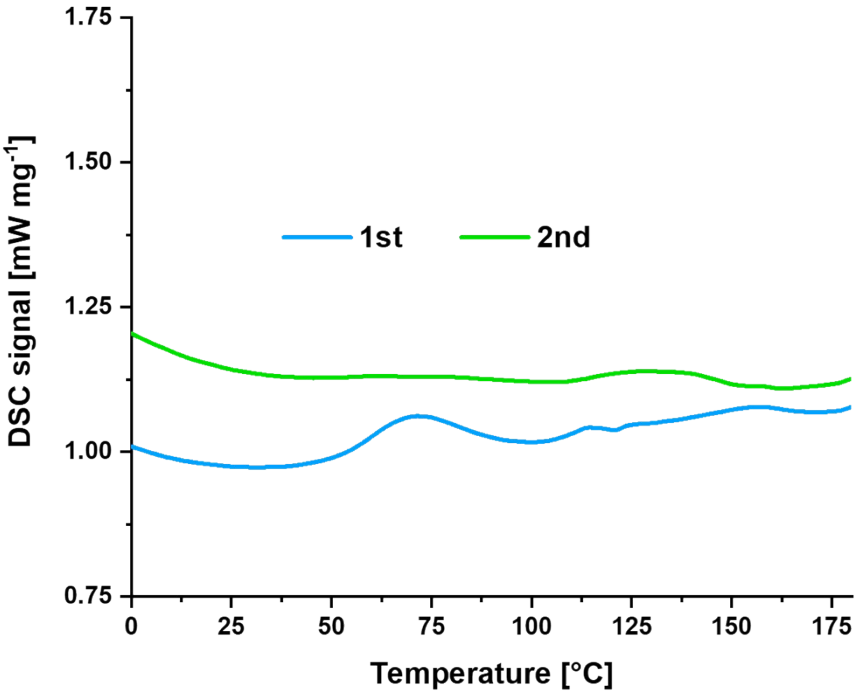

Figure S12. DSC-curves of the first (blue) and second (green) heating cycle of **IPN-5**.

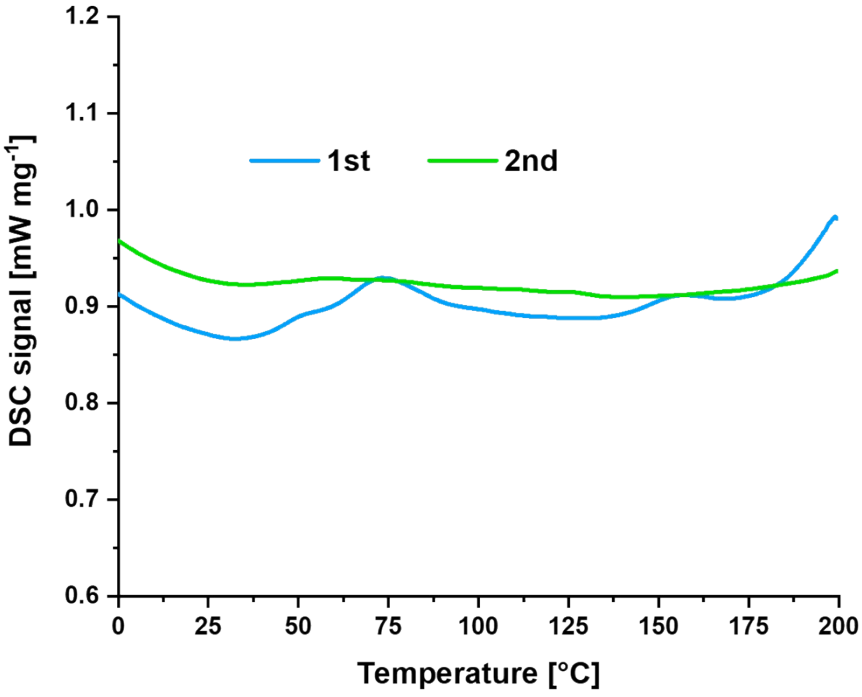

Figure S13. DSC-curves of the first (blue) and second (green) heating cycle of **IPN-6**.

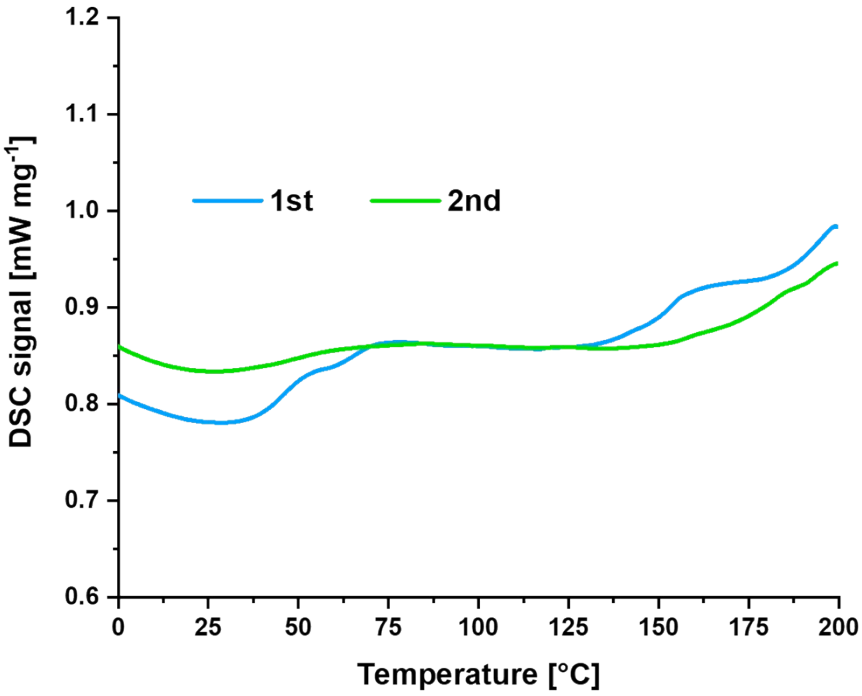

Figure S14. DSC-curves of the first (blue) and second (green) heating cycle of **IPN-7**.

Thermo mechanical analyses (TMA)

Dual shape-memory

The sample was fixed into the rheometer (γ_A). The temperature was set to the switching temperature (T_{sw}). The metallopolymer network in its determined permanent shape (γ_A) was deformed at this temperature ($\gamma_{B,load.}$) (tuning in linear ramp) until the shear stress reached the shear stress value, which corresponds to a deformation of about 120° (this value was detected in a prior measurement at the same temperature). Subsequently, the sample was cooled to 30 °C (cooling rate: 2 to10 K min^{-1}) under constant shear stress to fix the temporary shape. Thereafter, the release of the shear stress (to 0 Pa) was performed (γ_B). For the recovery, the sample was heated again to the initial temperature (heating rate: 10 K min^{-1}) followed by an annealing step at this temperature leading to the recovery of the permanent shape ($\gamma_{A,rec.}$). The measurement was in general repeated three times without interruptions. The results are summarized in **Table S5**.

Table S5. Results of the thermo-mechanical analyses of the interpenetrating metallopolymer networks **IPN-1** to **IPN-7**.

	T_{sw} [°C]	Cycle	γ_A [%]	$\gamma_{B,load}$ [%]	γ_B [%]	$\gamma_{A,rec}$ [%]	R_f [%]	R_r [%]
IPN-1	90	1	0	25.3	24.9	3.7	98.4	85.4
		2	0	19.5	19.2	1.7	98.5	91.3
		3	0	17.6	17.2	1.2	97.7	93.2
		4	0	16.5	16.2	1.0	98.2	93.9
IPN-2	70	1	0	25.2	25.0	2.8	99.2	88.9
		2	0	21.9	21.6	0.9	98.6	95.9
		3	0	20.7	20.3	0.6	98.1	97.1
		4	0	20.1	19.6	0.4	97.5	98.0
IPN-3	80	1	0	29.0	28.5	4.7	98.3	83.8
		2	0	22.7	22.1	1.9	97.4	91.6
		3	0	20.2	19.7	1.2	97.5	94.1
		4	0	18.9	18.3	0.8	96.8	95.8
IPN-4	80	1	0	27.3	27.1	4.3	99.3	84.2
		2	0	24.3	24.1	2.8	99.2	88.5
		3	0	22.3	22.1	2.1	99.1	90.6
		4	0	21.0	20.8	1.8	99.0	91.4
IPN-5	80	1	0	30.7	30.5	3.3	99.3	89.3
		2	0	27.6	27.4	2.2	99.3	92.0
		3	0	25.8	25.6	1.8	99.2	93.0
		4	0	24.3	24.1	1.4	99.2	94.2
IPN-6	80	1	0	34.5	34.1	2.7	98.8	92.2
		2	0	29.6	29.2	1.4	98.6	95.3
		3	0	27.8	27.3	1.0	98.2	96.4
		4	0	26.6	26.2	0.8	98.5	97.0
IPN-7	80	1	0	37.2	36.7	1.3	98.7	96.5
		2	0	36.3	35.8	1.0	98.6	97.2
		3	0	36.4	35.8	0.8	98.4	97.8
		4	0	36.2	35.6	0.8	98.3	97.8

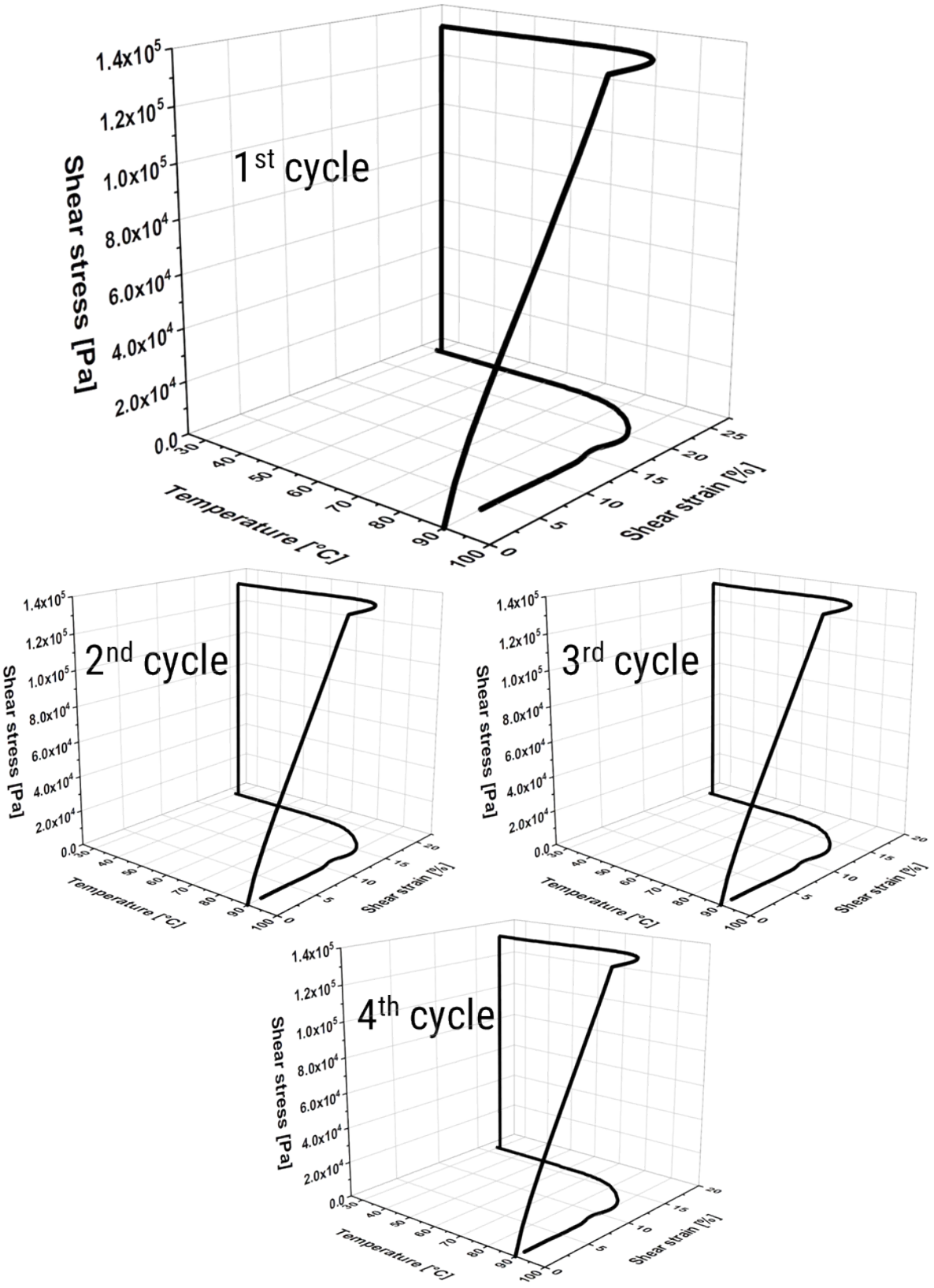

Figure S15. 3D-Plots of the thermo mechanical analysis of **IPN-1** at a switching temperature of 80 °C.

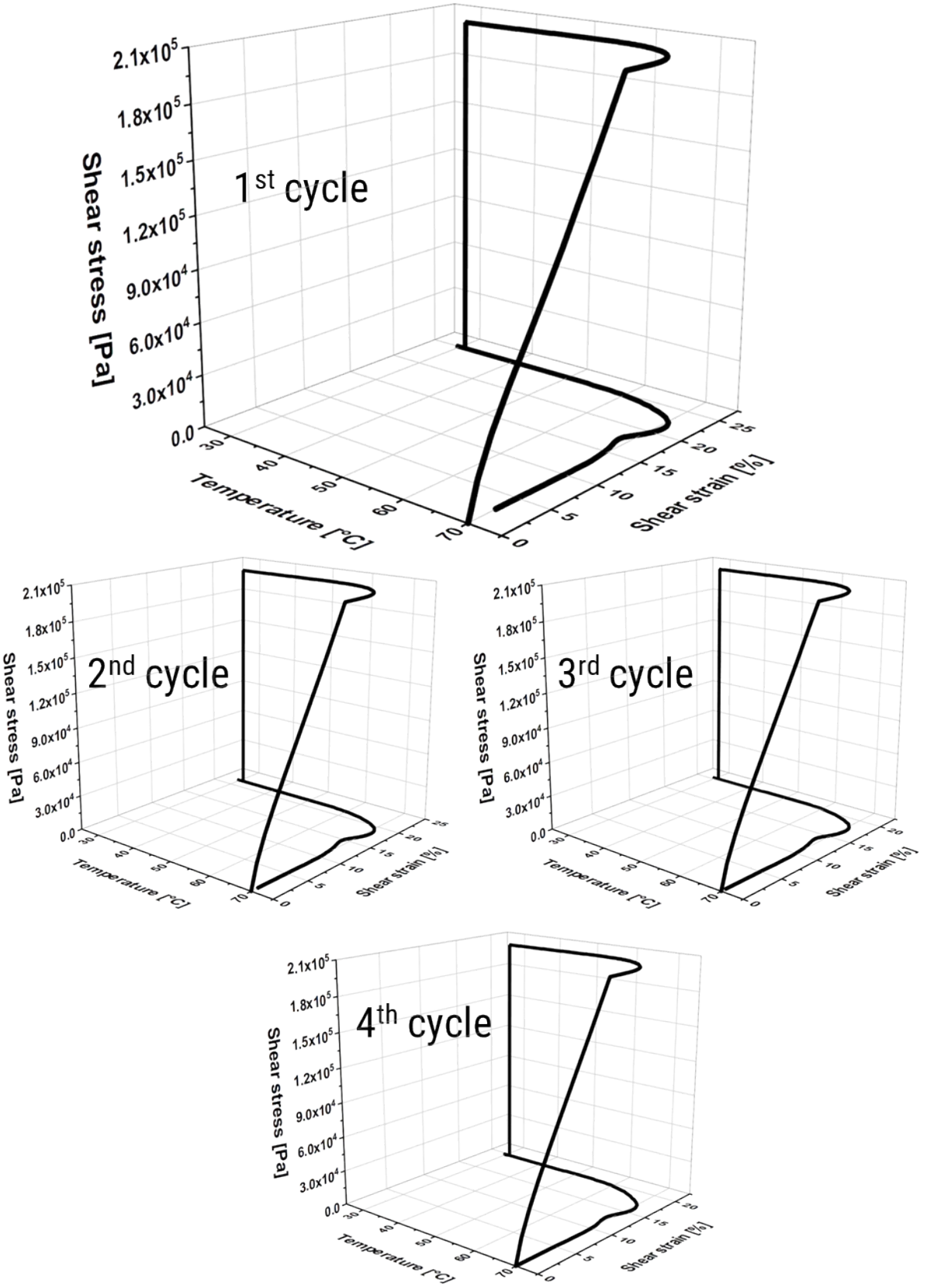

Figure S16. 3D-Plots of the thermo mechanical analysis of **IPN-2** at a switching temperature of 70 °C.

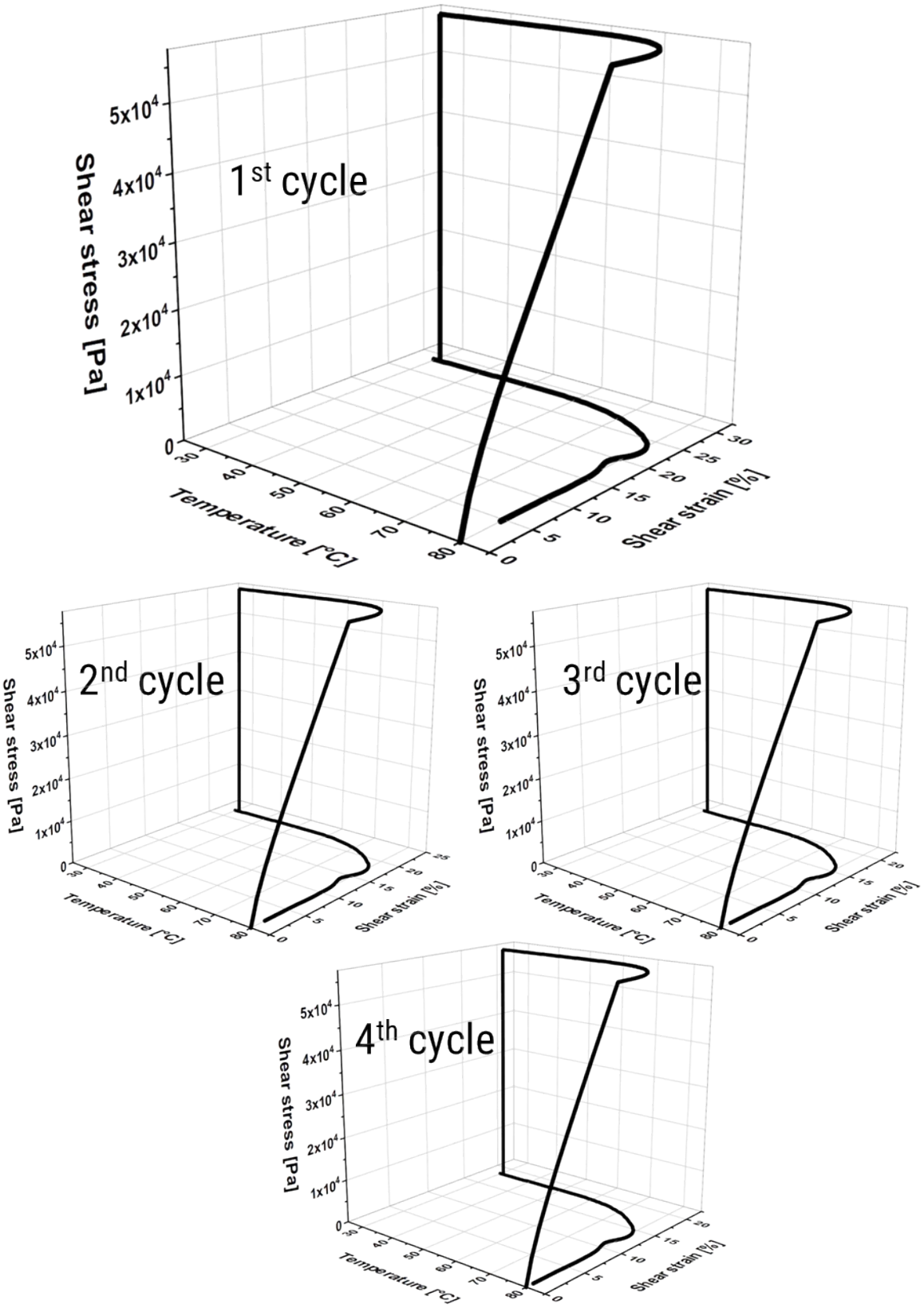

Figure S17. 3D-Plots of the thermo mechanical analysis of **IPN-3** at a switching temperature of 80 °C.

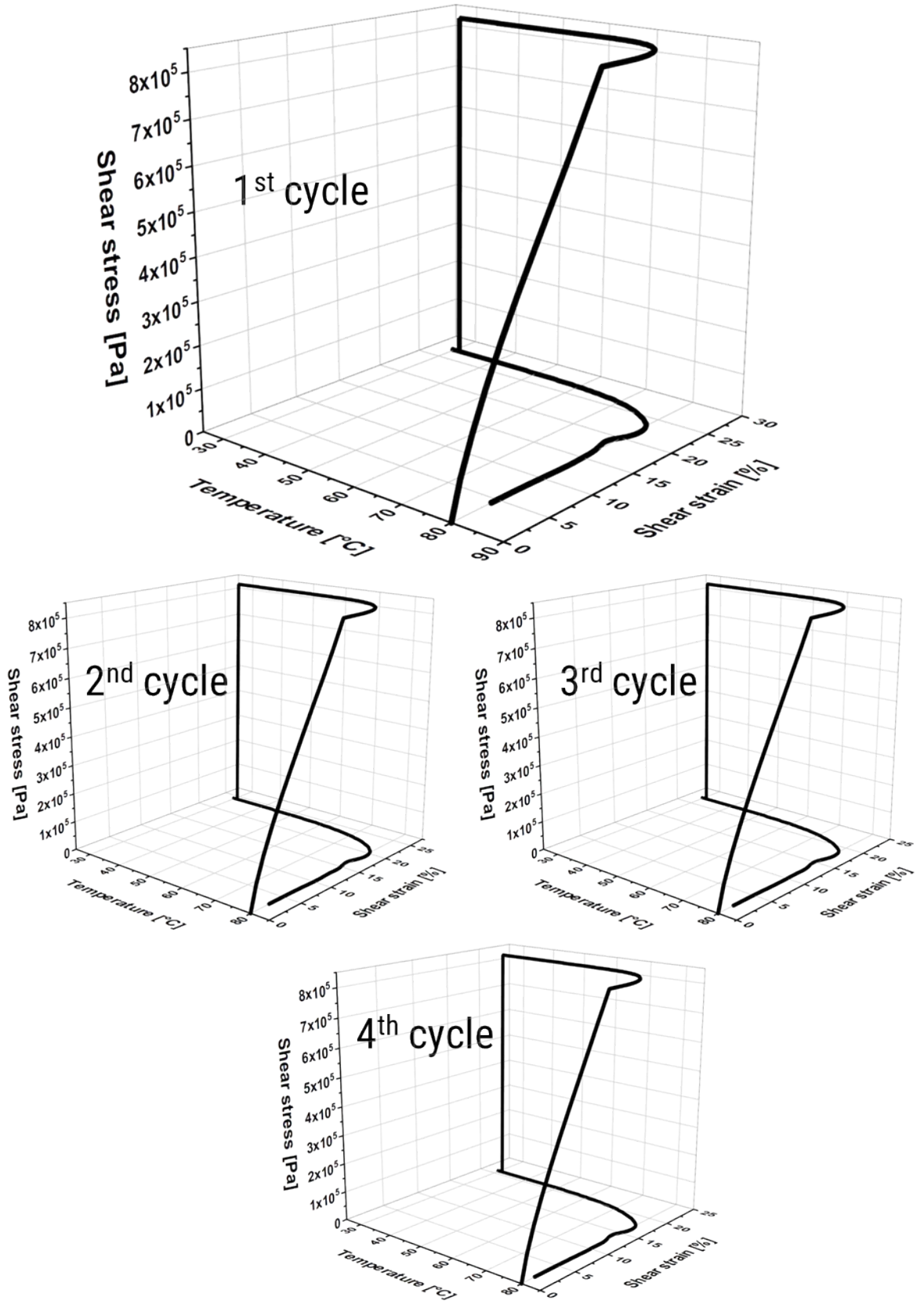

Figure S18. 3D-Plots of the thermo mechanical analysis of **IPN-4** at a switching temperature of 80 °C.

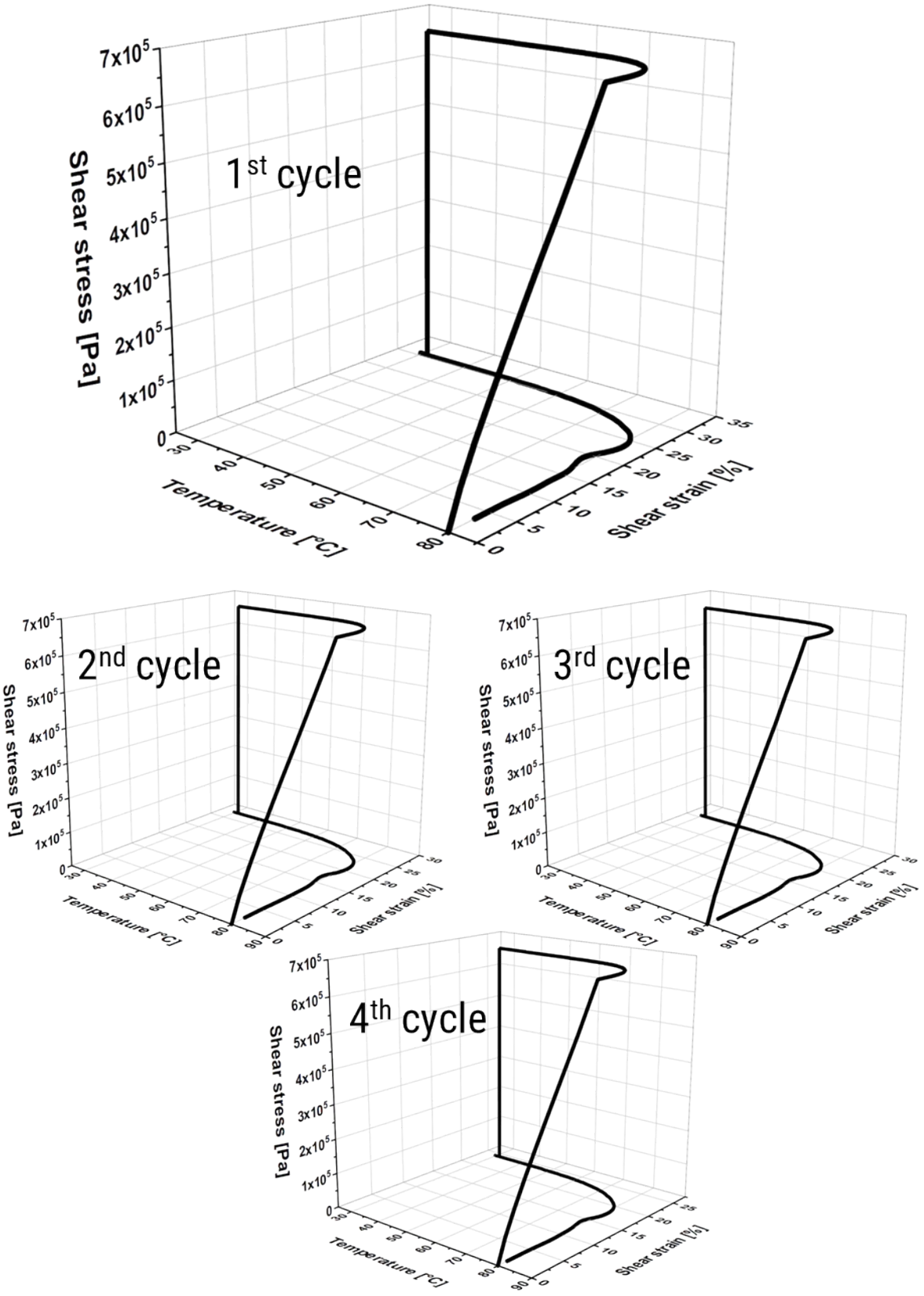

Figure S19. 3D-Plots of the thermo mechanical analysis of **IPN-5** at a switching temperature of 80 °C.

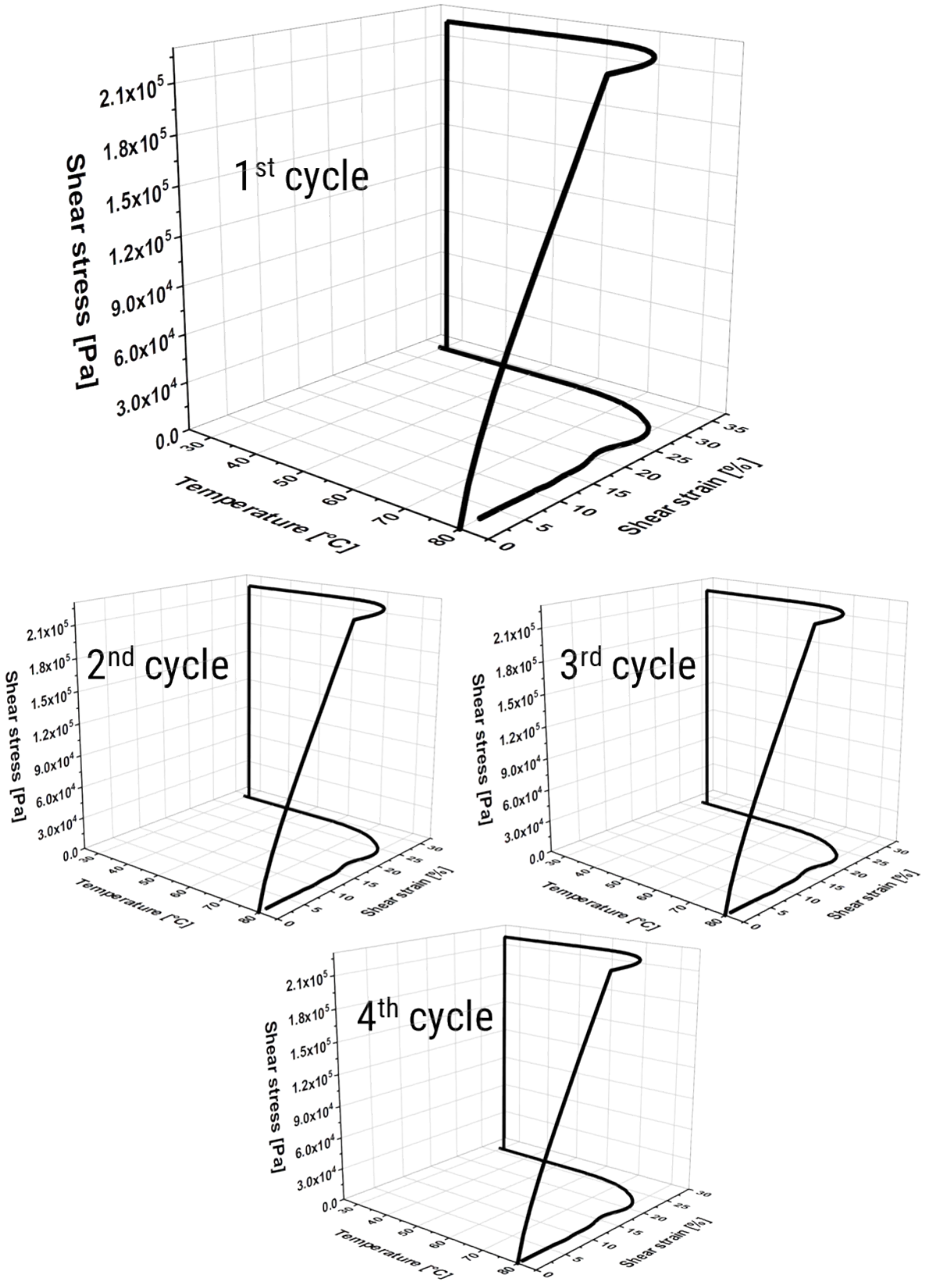

Figure S20. 3D-Plots of the thermo mechanical analysis of **IPN-6** at a switching temperature of 80 °C.

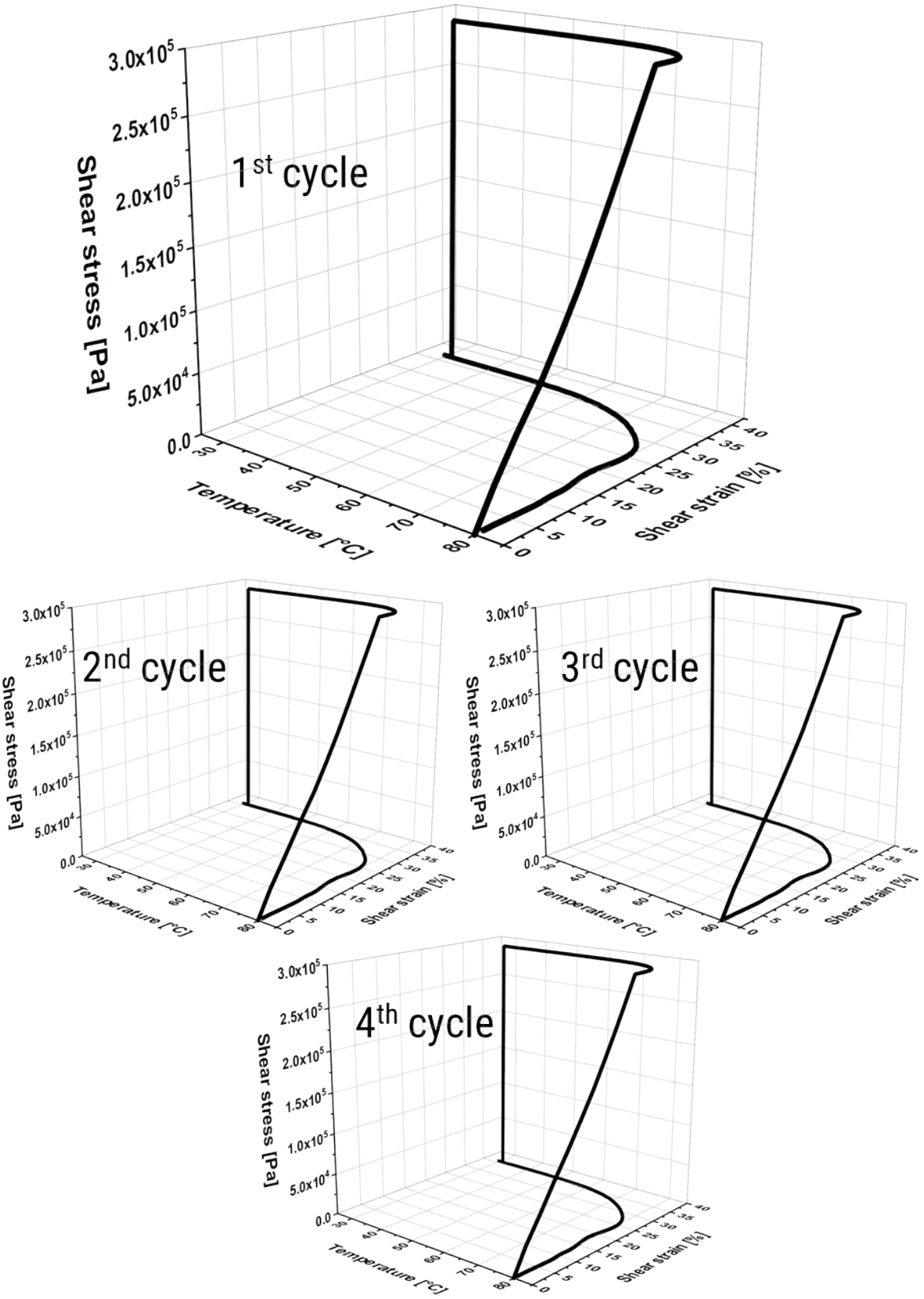

Figure S21. 3D-Plots of the thermo mechanical analysis of **IPN-7** at a switching temperature of 80 °C.

Rewriting

Additional analyses were performed to investigate the rewriting abilities of the metallopolymer networks and the corresponding shape-memory behavior afterwards. In the first steps of this investigation, a standard TMA cycle was performed (as described above). Afterwards, to rewrite the permanent shape, the sample was heated to 110 °C, and turned about 120° ($\gamma_{A2,load}$), followed by an annealing step at this temperature (1 h) while the deformation was kept constant. Afterwards, the sample was again cooled to the switching temperature and the stress was removed from the sample (γ_{A2}). After this rewriting step, again a TMA measurement was performed. The metallopolymer network in its rewritten permanent shape (γ_{A2}) was deformed at this temperature ($\gamma_{B2,load}$) (turning in linear ramp) until the shear stress reached the shear stress value, which corresponds to a deformation of about 120° (same value like first TMA). Subsequently, the sample was cooled to 30 °C (cooling rate: 2 to 10 K min^{-1}) under constant shear stress to fix the temporary shape. Thereafter, the release of the shear stress (to 0 Pa) was performed (γ_{B2}). For the recovery process, the sample was heated again to the initial temperature (heating rate: 15 K min^{-1}) followed by an annealing step at this temperature leading to the recovery of the rewritten permanent shape ($\gamma_{A2,rec.}$). This measurement was performed with all metallopolymer networks. The results are summarized in **Table S6**.

Table S6. Results of the thermo-mechanical analyses of the interpenetrating metallopolymer networks **IPN-1** to **IPN-7** for the investigation of the rewriting of the permanent shape and its influence on the shape-memory abilities.

	T_{sw} [°C]	γ_A [%]	$\gamma_{B,load}$ [%]	γ_B [%]	$\gamma_{A,rec}$ [%]	$\gamma_{A2,load}$ [%]	γ_{A2} [%]	$\gamma_{B2,load}$ [%]	γ_{B2} [%]	$\gamma_{A2,rec}$ [%]
IPN-1	90	0	15.0	14.4	1.0	–25.0	–22.7	11.6	10.9	–14.2
IPN-2	70	0	19.7	19.3	0.4	–25.0	–22.5	13.4	13.0	–17.8
IPN-3	80	0	28.8	28.3	1.8	–25.0	–23.2	24.5	24.0	–16.3
IPN-4	80	0	14.1	14.2	1.0	–25.0	–24.3	3.2	3.1	–20.4
IPN-5	80	0	31.2	31.0	3.67	–25.0	–23.9	26.3	26.0	–17.2
IPN-6	80	0	25.7	25.3	0.7	–25.0	–22.7	16.8	16.4	–18.8
IPN-7	80	0	15.0	14.4	1.0	–25.0	–18.5	35.8	35.1	–12.4

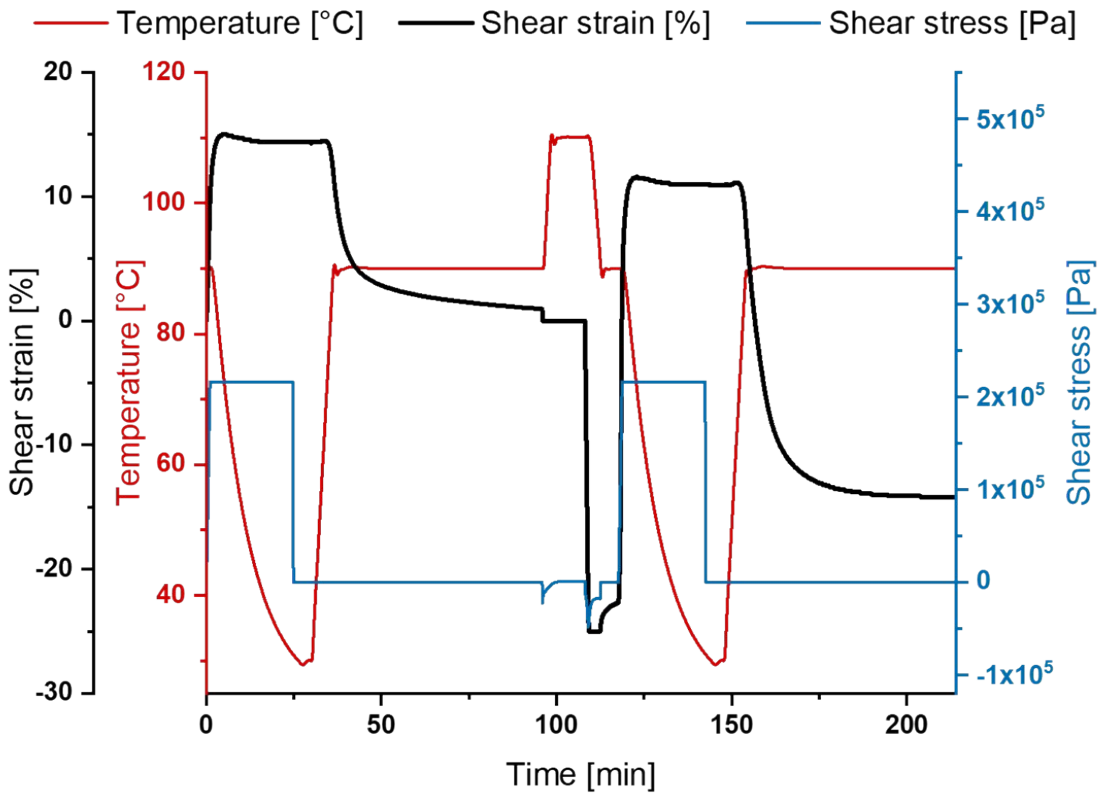

Figure S22. 2D-Plots of the thermo mechanical analysis of **IPN-1** for the investigation of the rewriting of the permanent shape and its influence on the shape-memory abilities.

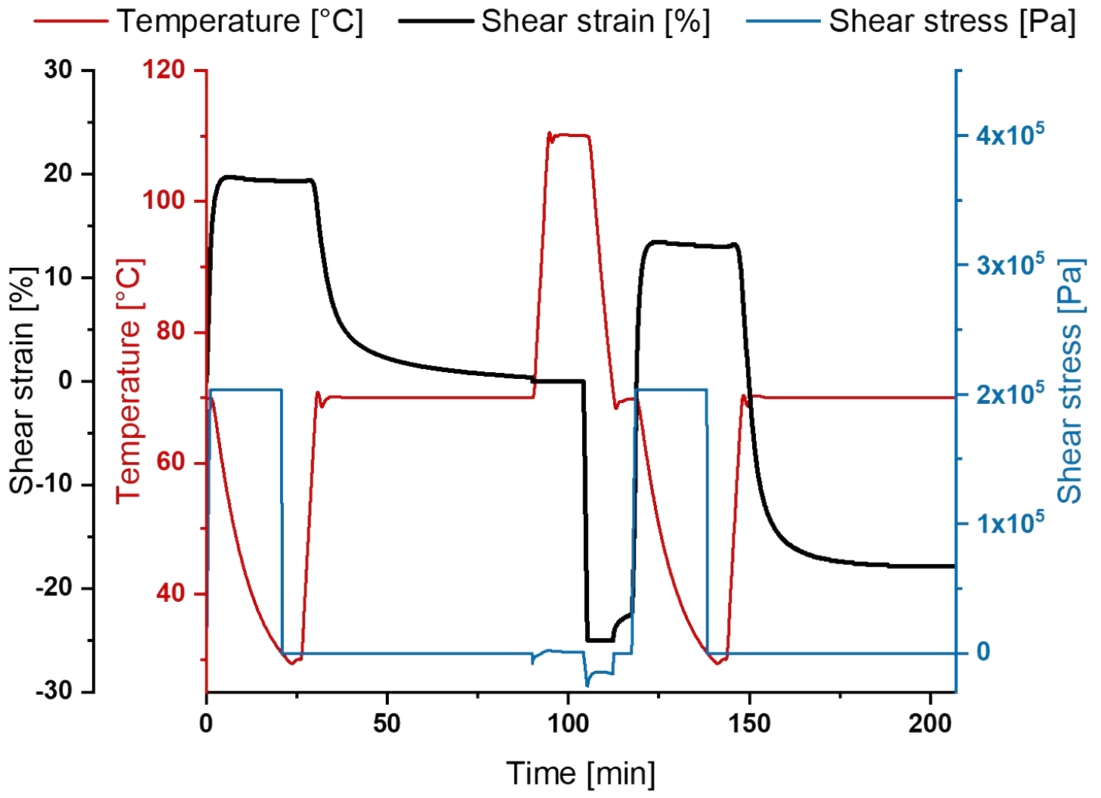

Figure S23. 2D-Plots of the thermo mechanical analysis of **IPN-2** for the investigation of the rewriting of the permanent shape and its influence on the shape-memory abilities.

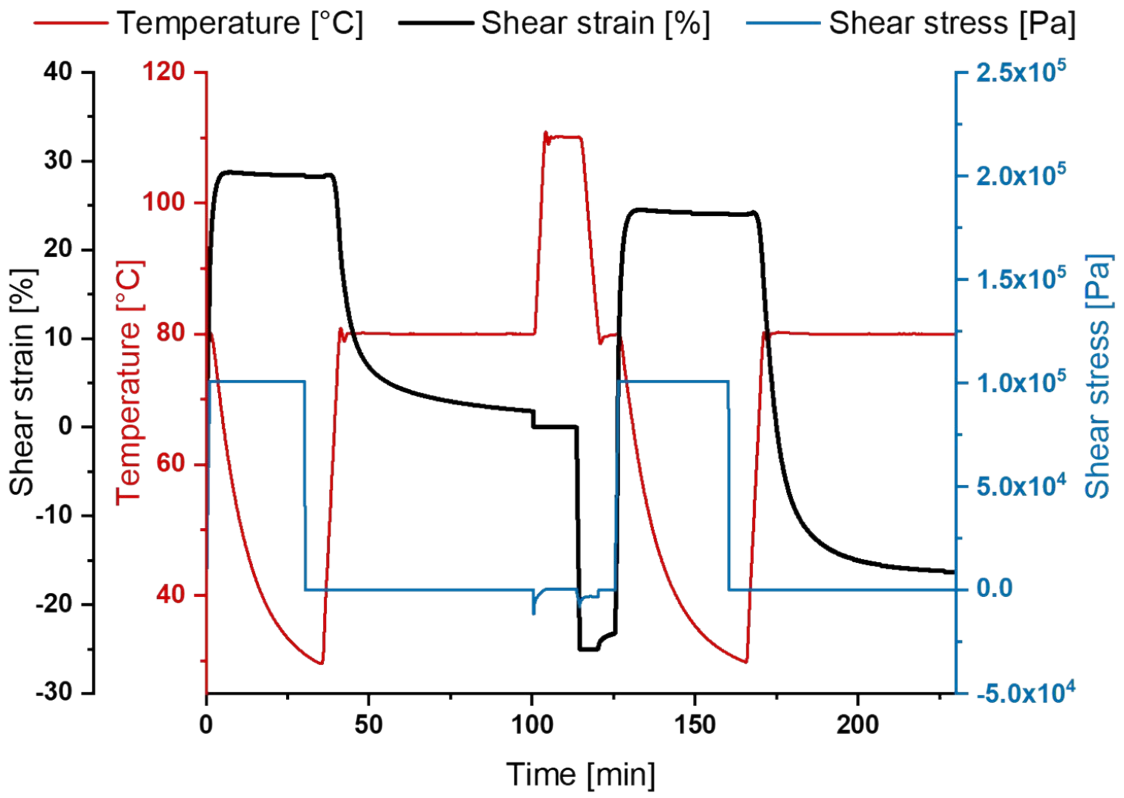

Figure S24. 2D-Plots of the thermo mechanical analysis of **IPN-3** for the investigation of the rewriting of the permanent shape and its influence on the shape-memory abilities.

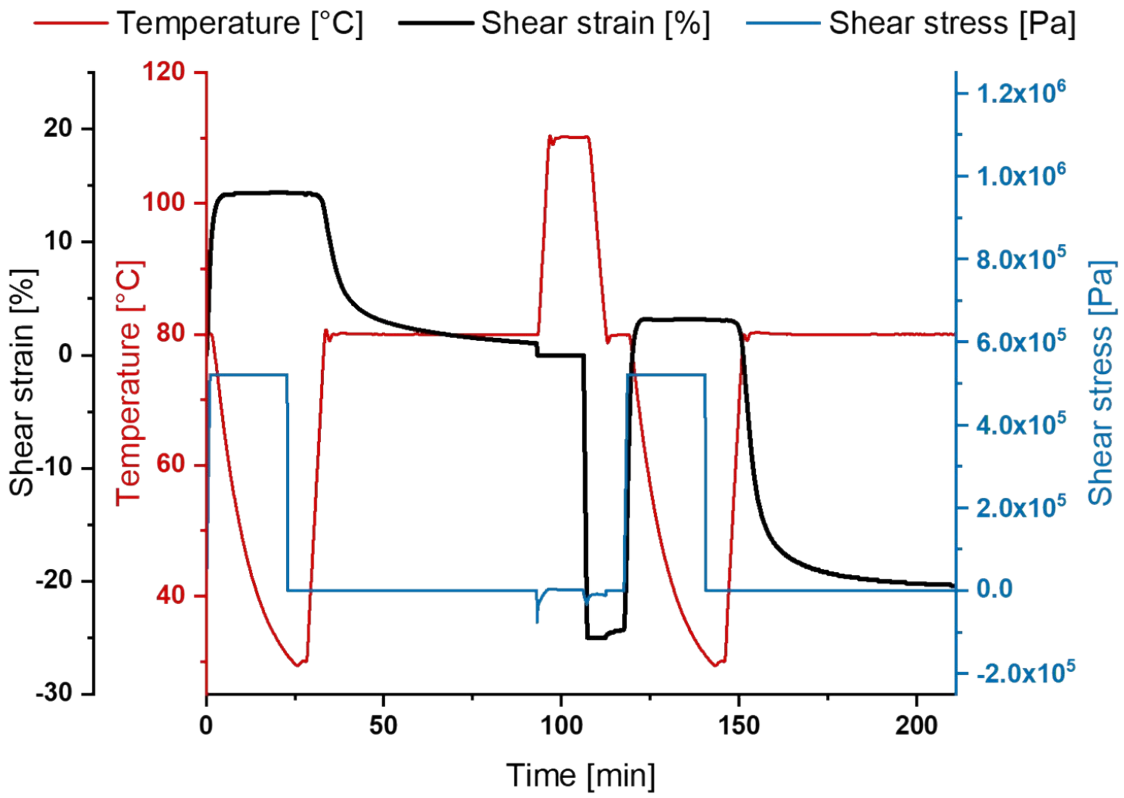

Figure S25. 2D-Plots of the thermo mechanical analysis of **IPN-4** for the investigation of the rewriting of the permanent shape and its influence on the shape-memory abilities.

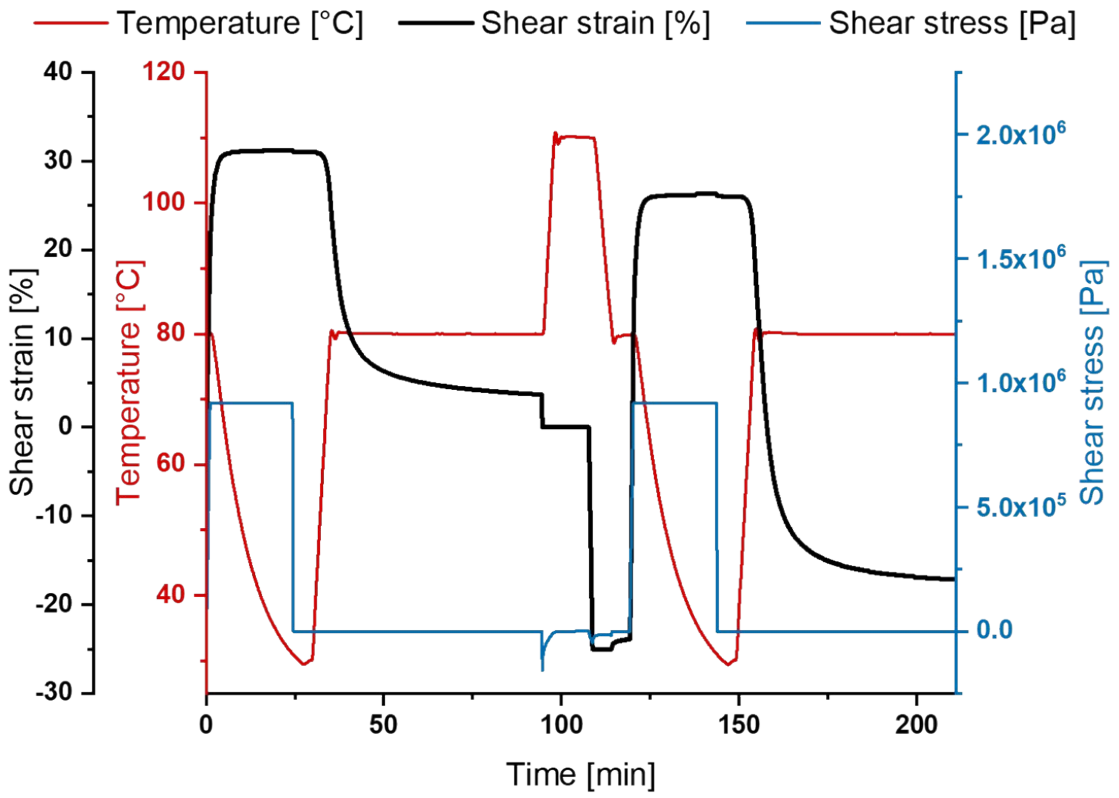

Figure S26. 2D-Plots of the thermo mechanical analysis of **IPN-5** for the investigation of the rewriting of the permanent shape and its influence on the shape-memory abilities.

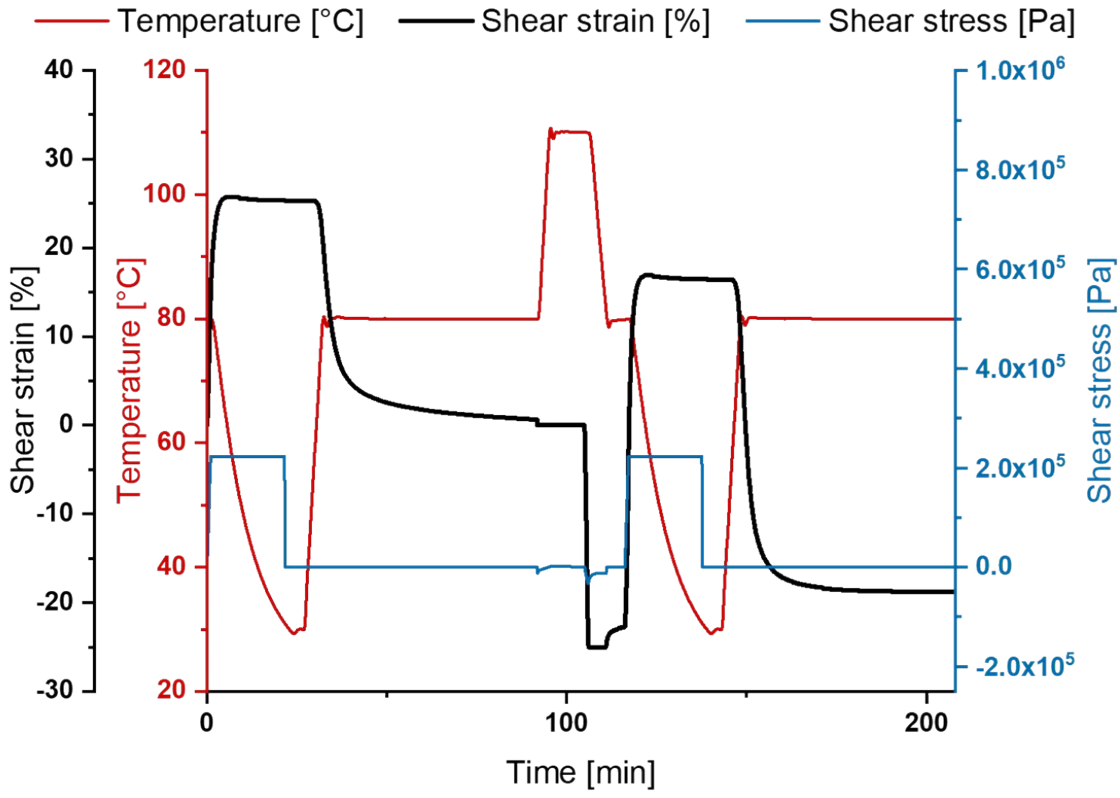

Figure S27. 2D-Plots of the thermo mechanical analysis of **IPN-6** for the investigation of the rewriting of the permanent shape and its influence on the shape-memory abilities.

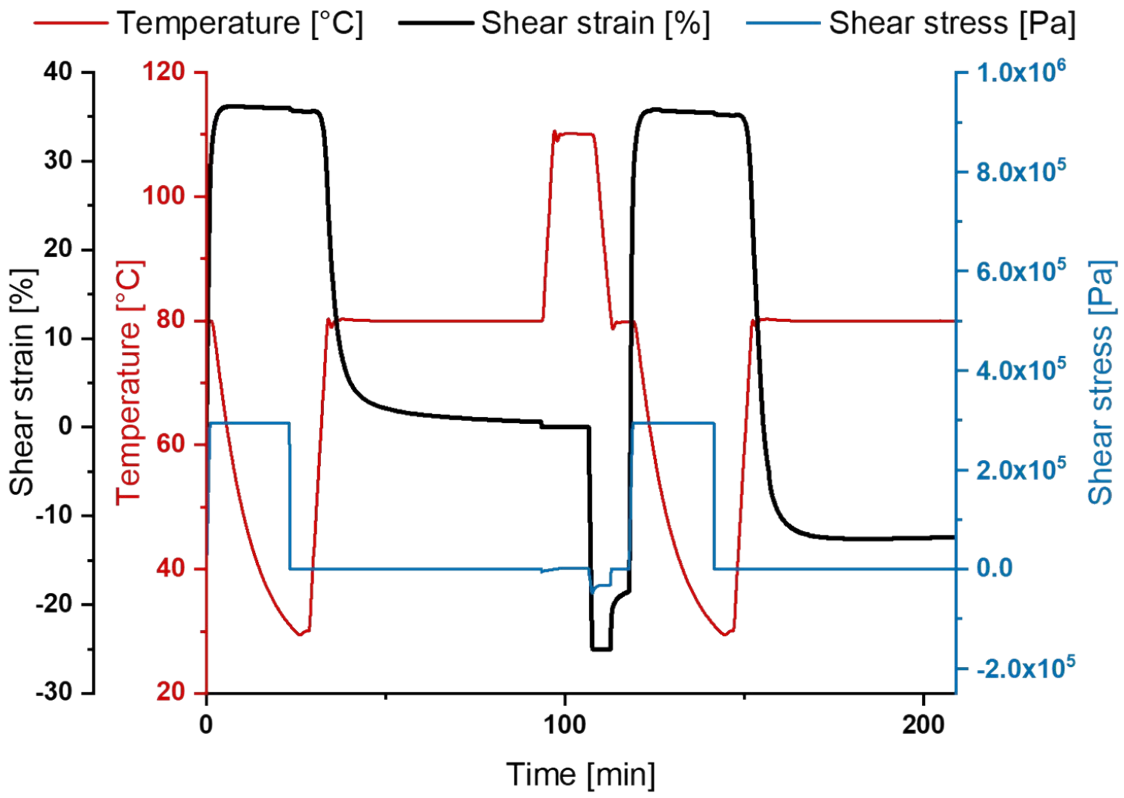

Figure S28. 2D-Plots of the thermo mechanical analysis of **IPN-7** for the investigation of the rewriting of the permanent shape and its influence on the shape-memory abilities.

Self-healing experiments

Self-healing studies were performed according to literature procedures.[3, 4] In the first step, the sample was pressed analogously to the samples for the shape-memory tests in a special manufactured mold resulting in round, flat samples. The pressed polymer samples were embedded in epoxy resin consisting of Epoxy Resin L and Hardener CL from R&G Faserverbundstoffe GmbH. Followed by grinding of the sample with sandpaper (P60 to P2500). The self-healing scratch tests were performed on an Anton Paar Micro scratch tester MST^3 on a STeP 4 platform. The instrument was equipped with 10 µm and 50 µm Rockwell C indenters and the optical images were taken with the lenses MPlan N 5×/0.10/FN22 and MPlan N 20×/0.40/FN22. The scratches were generated with a 50 µm Rockwell indenter, 1500 mN normal force and 15 passages on a length of 2000 µm and a scratch speed of 30000 µm min^{-1}. Subsequently, the scratch was imaged by the microscope in panorama mode. The sample was turned about an angle of 90° in order to measure the profile of the scratches. Therefore, 140 scratches along the scratch (every 20 µm) were performed with a 10 µm Rockwell indenter with the following parameters: 3 mN normal force, 200 µm min^{-1} scratch speed, length 800 µm.

For the visualization and evaluation of the scratch profile data recorded by the MST^3, a Python-based GUI controlled program, which mainly uses the well-established data analysis library *pandas* as well as the *SciPy* and *NumPy* libraries for linear algebra, integration and interpolation, was utilized.

Table S7. Determined scratch volumes (under the surface) and calculated healing efficiencies (H_{eff}) for the interpenetrating networks **IPN-1** to **IPN-6**.

	Salt in P1	**Salt in P2**	**Ratio P1 to P2**	**Scratch volume [µm³]**	**Volume after 24 h at 140 °C [µm³]**	**H_{eff} [%]**
IPN-1	$Zn(TFMS)_2$		2 : 1	– 9,358,334.22	– 182,695,25	98.0
IPN-2	$FeSO_4$		2 : 1	– 18,736,347.49	– 6,425,591,71	65.7
IPN-3	$NiCl_2$	$FeSO_4$	2 : 1	– 16,105,622.88	– 13,182,313,58	18.2
IPN-4	$Zn(TFMS)_2$	$NiCl_2$	2 : 1	– 9,598,182.97	– 10,423,906,47	– 8.6
IPN-5	$Zn(TFMS)_2$	$FeSO_4$	2 : 1	– 11,104,410.47	– 2,169,762.83	79.0
IPN-6	$Zn(TFMS)_2$	$FeSO_4$	1 : 1	– 12,807,769.78	– 4,355,274.88	66.0

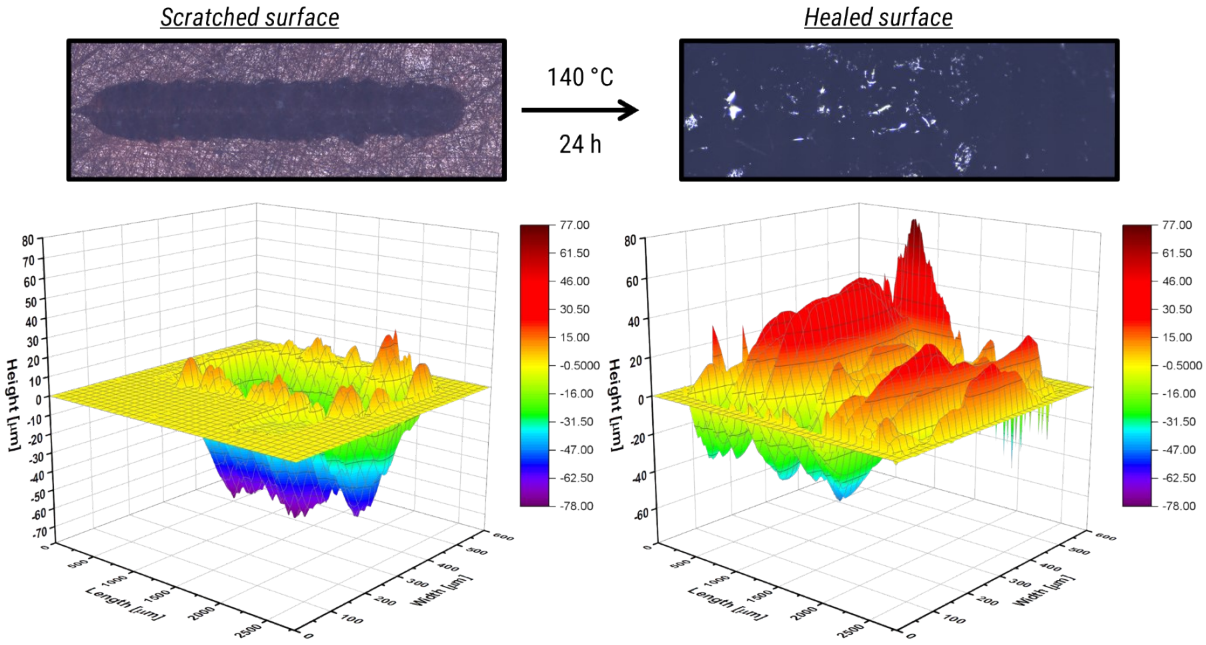

Figure S29. Optical images (top) and 3D-plot of the profile measurement (bottom) of **IPN-2** during the performed scratch-healing test (left: Surface with scratch; right: Surface after healing for 24 h at 140 °C).

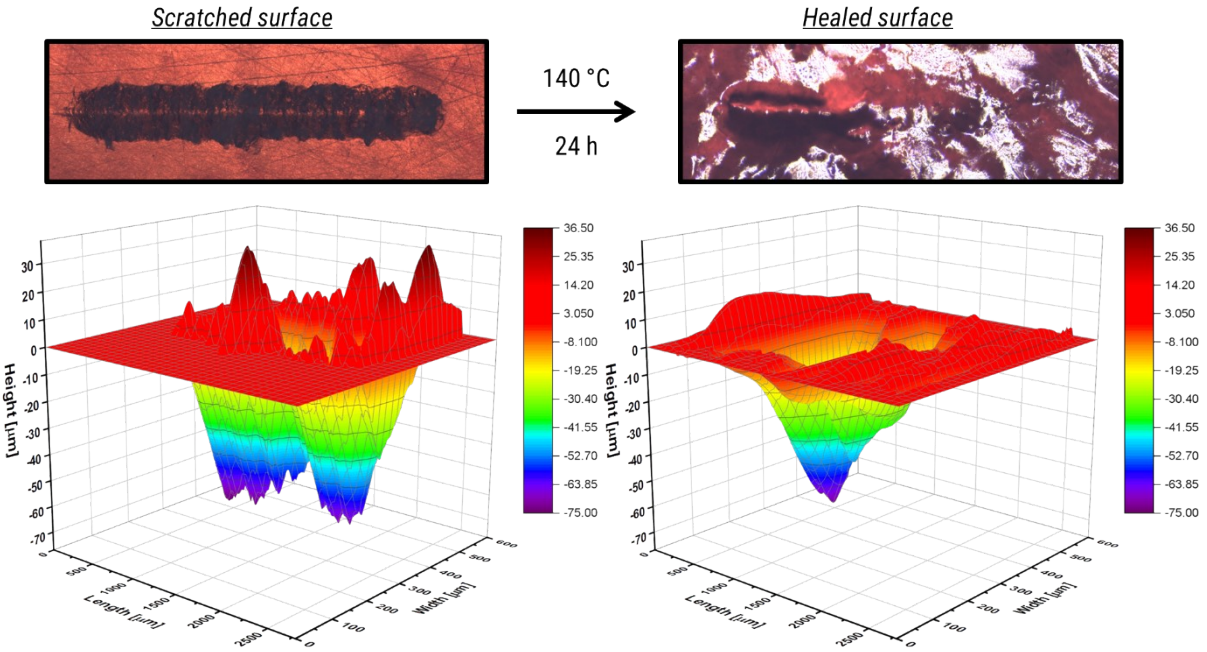

Figure S30. Optical images (top) and 3D-plot of the profile measurement (bottom) of **IPN-3** during the performed scratch-healing test (left: Surface with scratch; right: Surface after healing for 24 h at 140 °C).

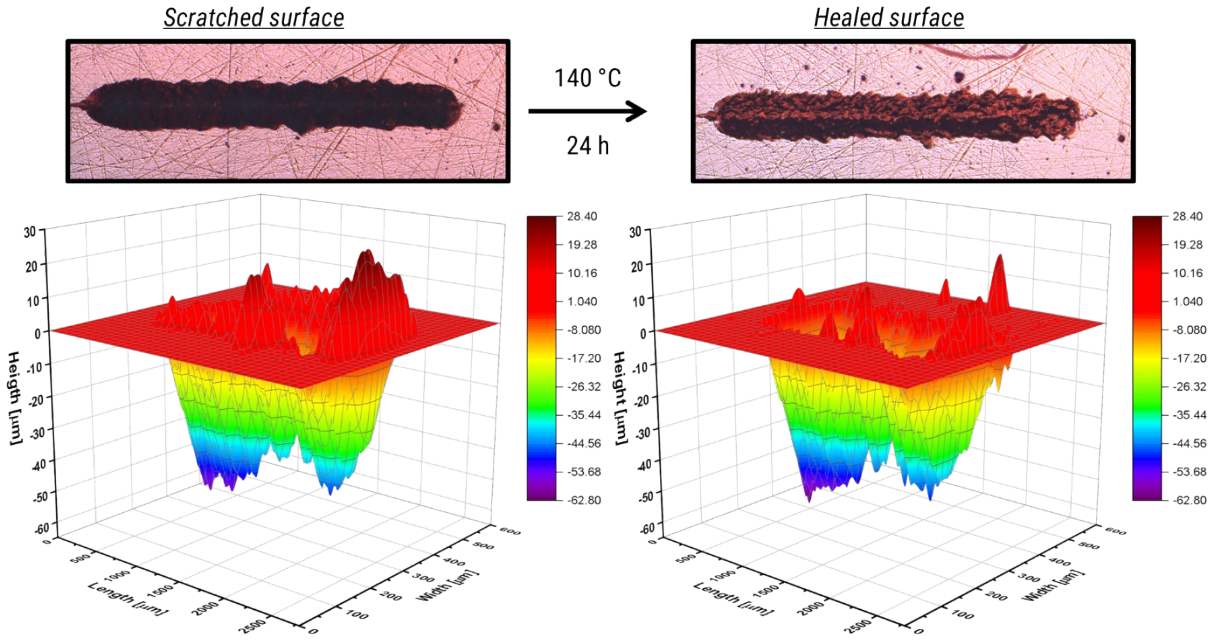

Figure S31. Optical images (top) and 3D-plot of the profile measurement (bottom) of **IPN-4** during the performed scratch-healing test (left: Surface with scratch; right: Surface after healing for 24 h at 140 °C).

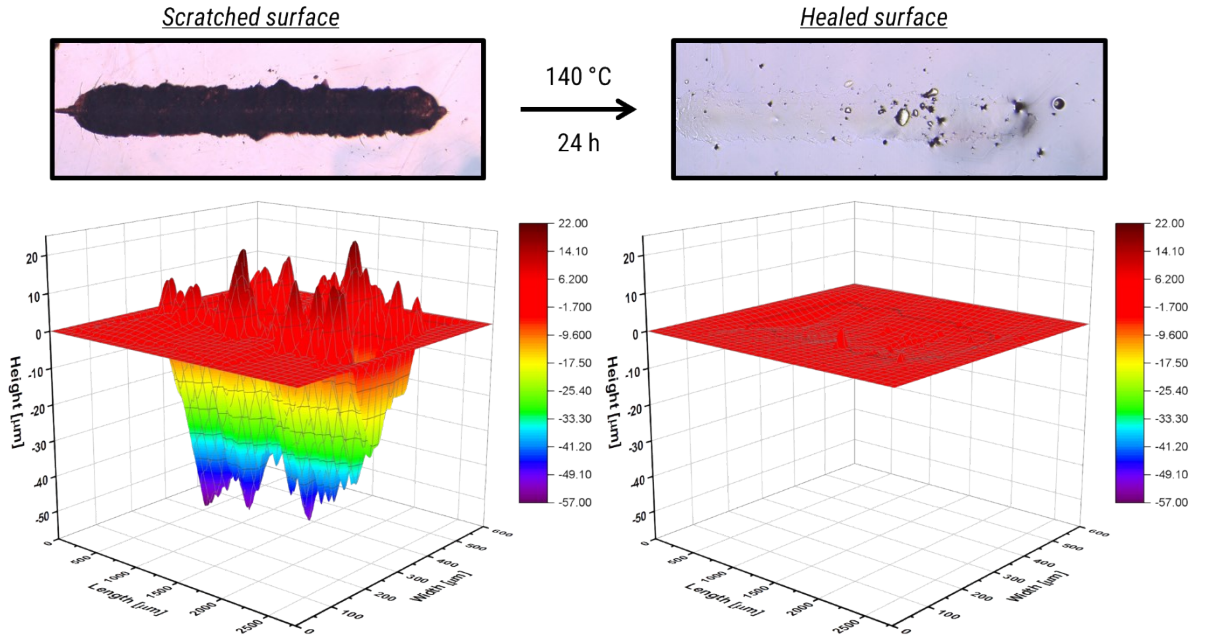

Figure S32. Optical images (top) and 3D-plot of the profile measurement (bottom) of **IPN-5** during the performed scratch-healing test (left: Surface with scratch; right: Surface after healing for 24 h at 140 °C).

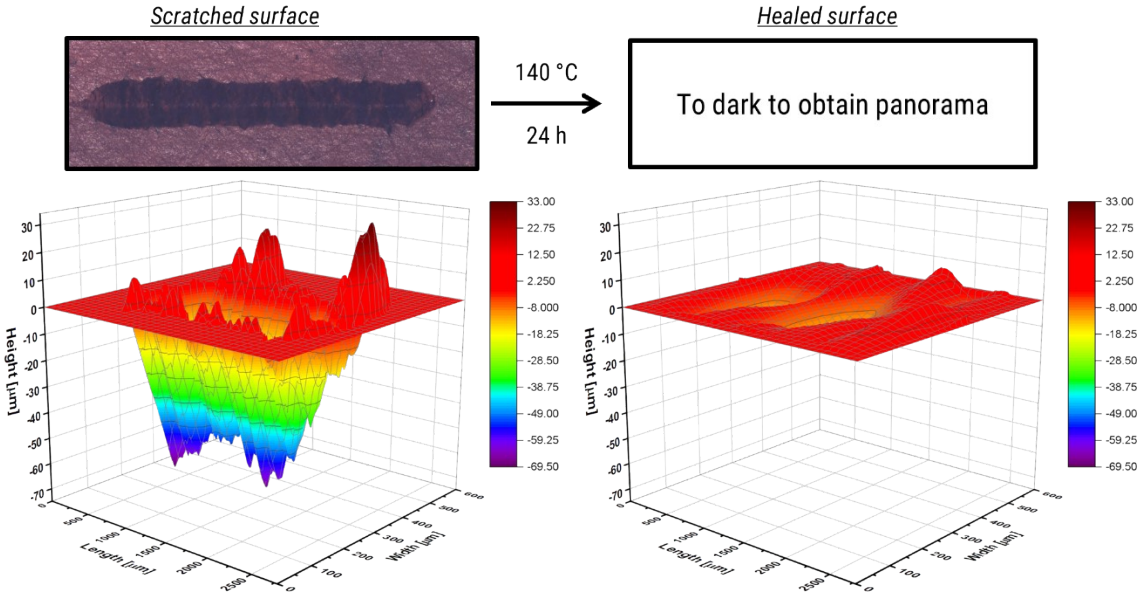

Figure S33. Optical images (top) and 3D-plot of the profile measurement (bottom) of **IPN-6** during the performed scratch-healing test (left: Surface with scratch; right: Surface after healing for 24 h at 140 °C).

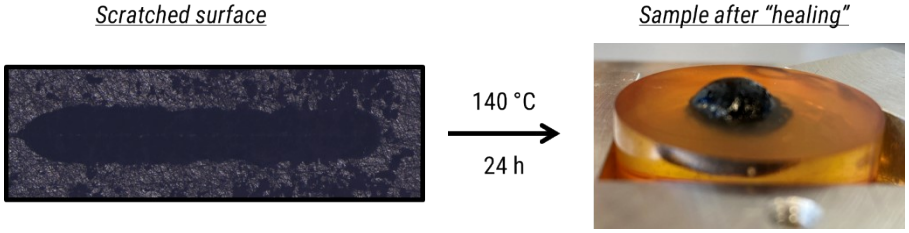

Figure S34. Optical images of the scratched surface of **IPN-7** (left) and photo of the sample **IPN-7** after annealing for 24 h at 140 °C (right).

FT-Raman spectroscopy

Table S8. Laser power at sample and number of accumulated scans for the FT-Raman measurements of all samples.

Sample	Power / mW	Scans	Sample	Power / mW	Scans
P1	500	128	**IPN-1**	300	128
P1-Fe	500	128	**IPN-2**	300	128
P1-Zn	500	128	**IPN-3**	300	128
P1-Ni	100	1024	**IPN-4**	500	128
P2	500	128	**IPN-5**	500	128
P2-Fe	500	128	**IPN-6**	500	128
P2-Zn	500	128	**IPN-7**	500	128
P2-Ni	500	128			

For further evaluation the raw Raman data was preprocessed using R 4.1.2.[3] The spectra were restricted to the wavenumber of interest (200 to 3200 cm^{-1}) followed by background correction using the SNIP-algorithm (iterations: 60, order: 3, smoothing window: 3) and normalized using euclidean vector norm.[4]

Table S9. Band positions of characteristic bands for free and bound Tpy and *trt*-His for the model polymers **P1** and **P2** as well as the interpenetrating networks **IPN1** to **IPN-7**.

Sample	Metal Salt(s)	Band Position / cm^{-1}			
		δC−C/C−N (Tpy)	νC−N (*trt*-His)	νC=C (Tpy)	
P1	-	-	1358	-	-
P1-Fe	$FeSO_4$	-	1360-1364, br	-	-
P1-Zn	$Zn(TFMS)_2$	-	1371	-	-
P1-Ni	$NiCl_2$	-	1366	-	-
P2	-	997	-	1574	1601
P2-Fe	$FeSO_4$	1021	-	1562	1601-1620, br
P2-Zn	$Zn(TFMS)_2$	1021	-	1563	1604
P2-Ni	$NiCl_2$	1020	-	1559	1604
IPN-1	$Zn(TFMS)_2$	1021	1371	1563	1603
IPN-2	$FeSO_4$	1021	1364	1561	1605, br
IPN-3	$NiCl_2$ / $FeSO_4$	1020	1366	1561	1602
IPN-4	$Zn(TFMS)_2$ / $NiCl_2$	1021	1369	1562	1603
IPN-5	$Zn(TFMS)_2$ / $FeSO_4$	1021	1368	1562	1603
IPN-6	$Zn(TFMS)_2$ / $FeSO_4$	1021	1366	1563	1604
IPN-7	$Zn(TFMS)_2$ / $FeSO_4$	1021	1364	1563	1605, br

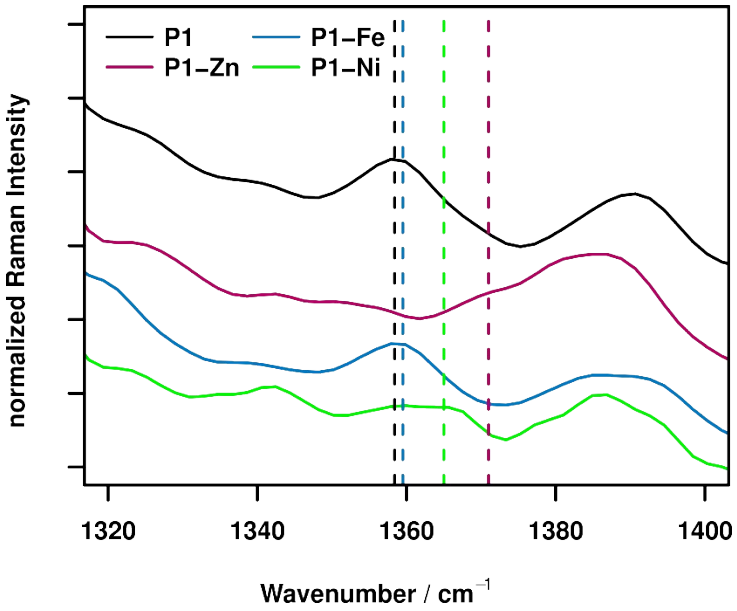

Figure S35. FT-Raman spectra of model polymer **P1** and its derivatives produced by addition of $FeSO_4$ (**P1-Fe**), $NiCl_2$ (**P1-Ni**) and $Zn(TFMS)_2$ (**P1-Zn**) in the C-N stretching region.

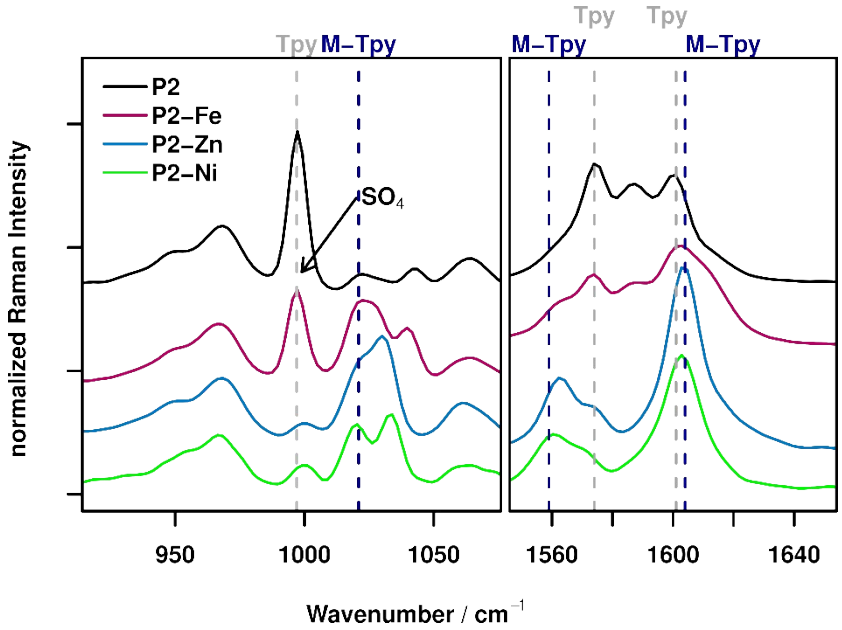

Figure S36. FT-Raman spectra of model polymer **P2** and its derivatives produced by addition of $FeSO_4$ (**P2-Fe**), $NiCl_2$ (**P2-Ni**) and $Zn(TFMS)_2$ (**P2-Zn**) in the C-C/C-N deformation region (left) as well as the C=C/C=N stretching region (right) of the terpyridine ligand in **P2**.

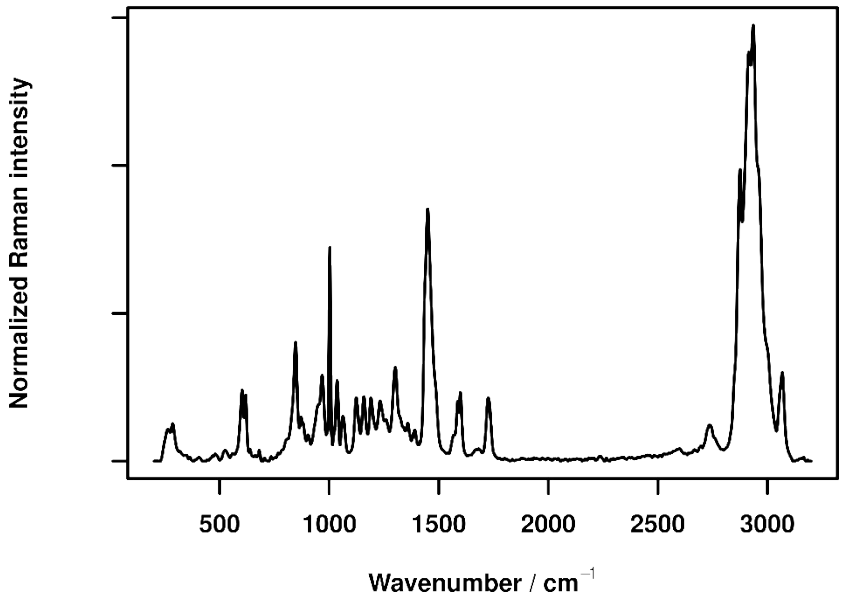

Figure S37. Normalized and background corrected (SNIP, 100 iterations, order 3) FT-Raman spectra of **P1** between 200 and 3200 cm^{-1}.

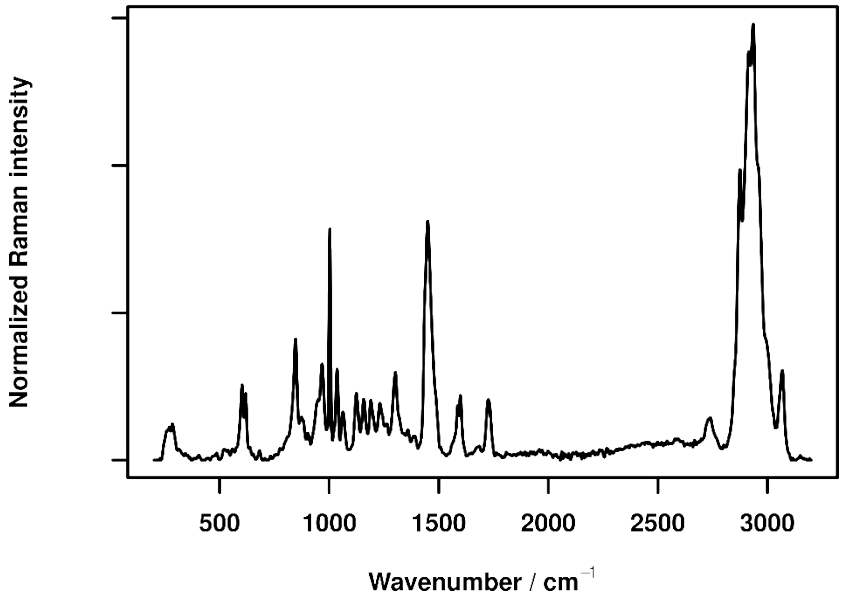

Figure S38. Normalized and background corrected (SNIP, 100 iterations, order 3) FT-Raman spectra of **P1-Fe** between 200 and 3200 cm^{-1}.

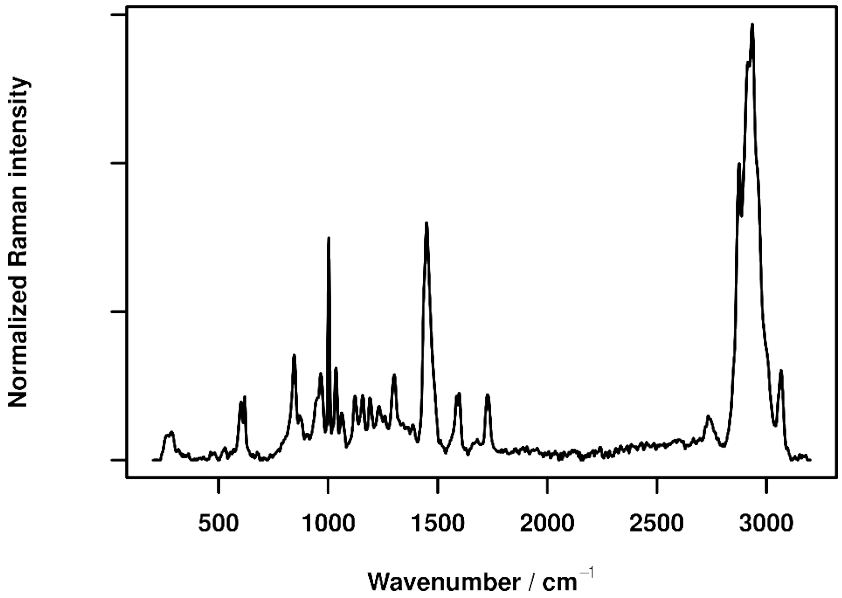

Figure S39. Normalized and background corrected (SNIP, 100 iterations, order 3) FT-Raman spectra of **P1-Ni** between 200 and 3200 cm^{-1}.

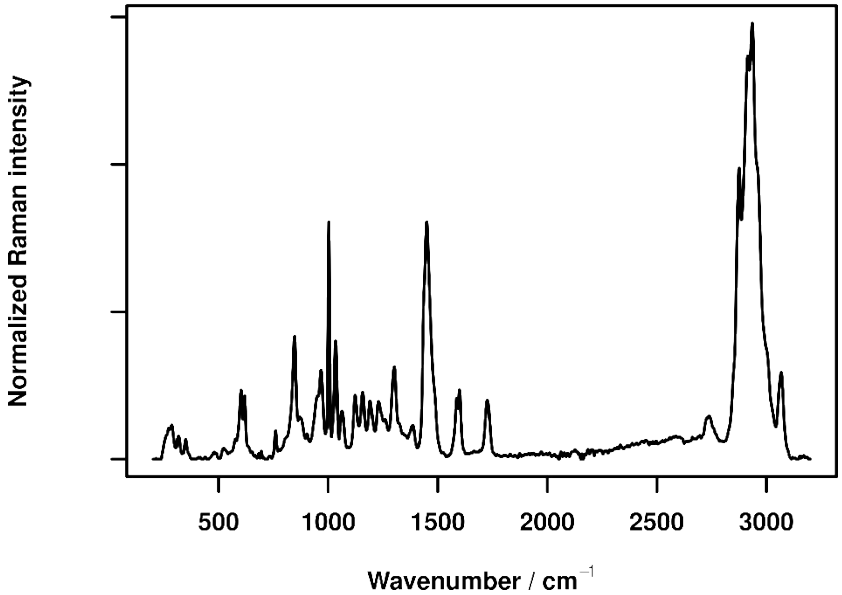

Figure S40. Normalized and background corrected (SNIP, 100 iterations, order 3) FT-Raman spectra of **P1-Zn** between 200 and 3200 cm^{-1}.

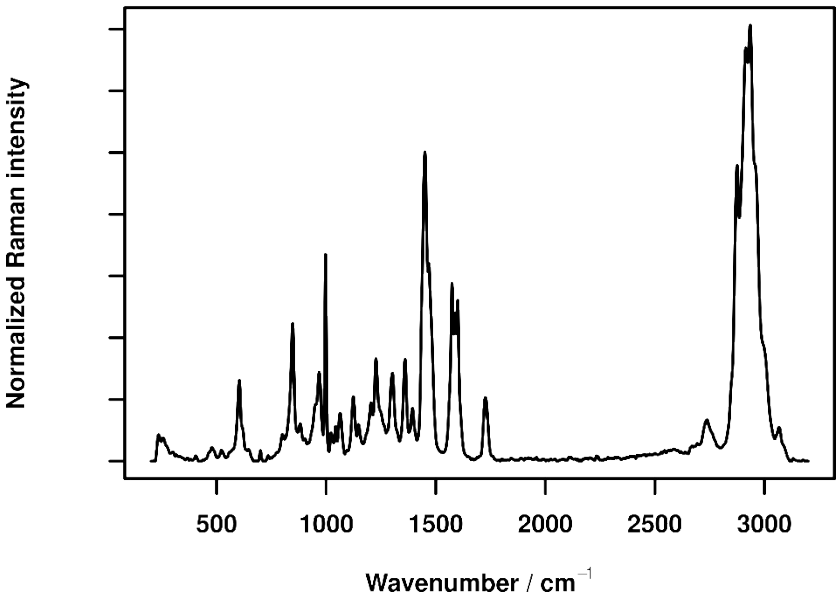

Figure S41. Normalized and background corrected (SNIP, 100 iterations, order 3) FT-Raman spectra of **P2** between 200 and 3200 cm^{-1}.

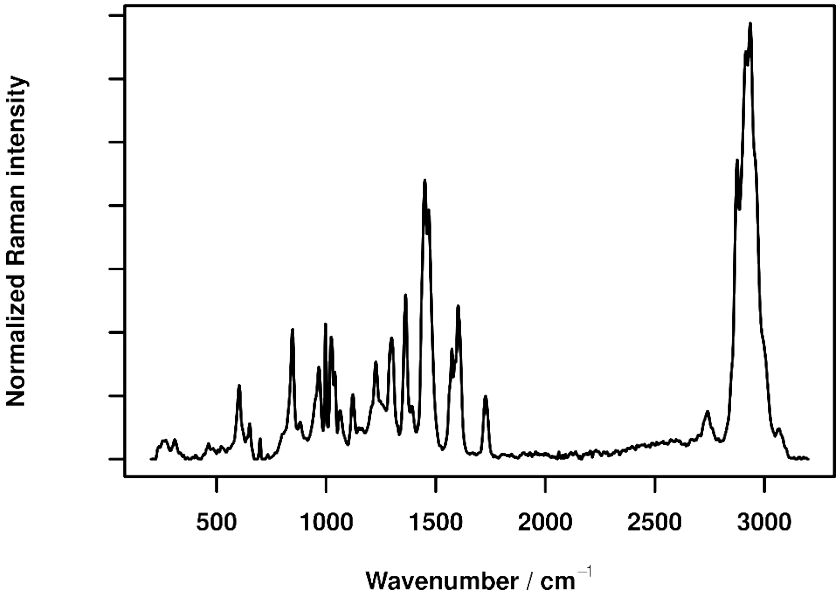

Figure S42. Normalized and background corrected (SNIP, 100 iterations, order 3) FT-Raman spectra of **P2-Fe** between 200 and 3200 cm^{-1}.

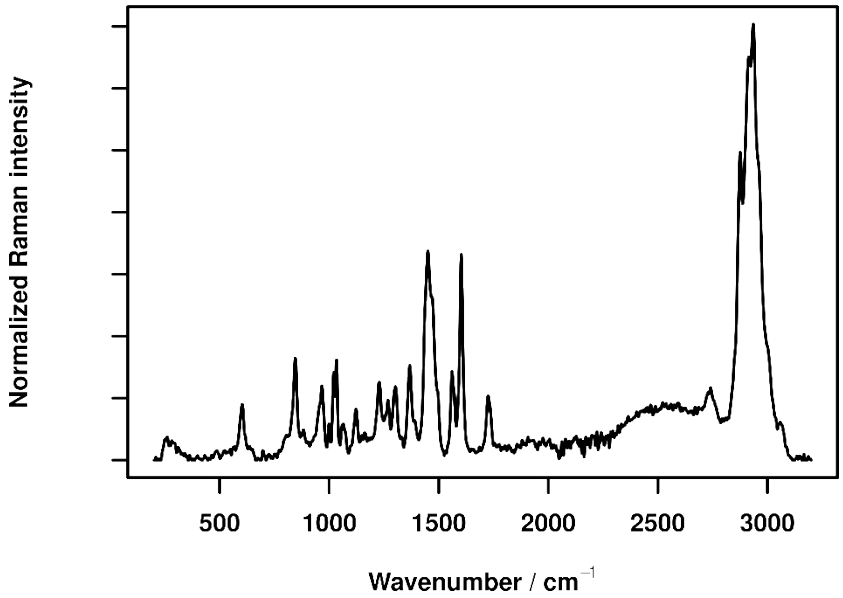

Figure S43. Normalized and background corrected (SNIP, 100 iterations, order 3) FT-Raman spectra of **P2-Ni** between 200 and 3200 cm^{-1}.

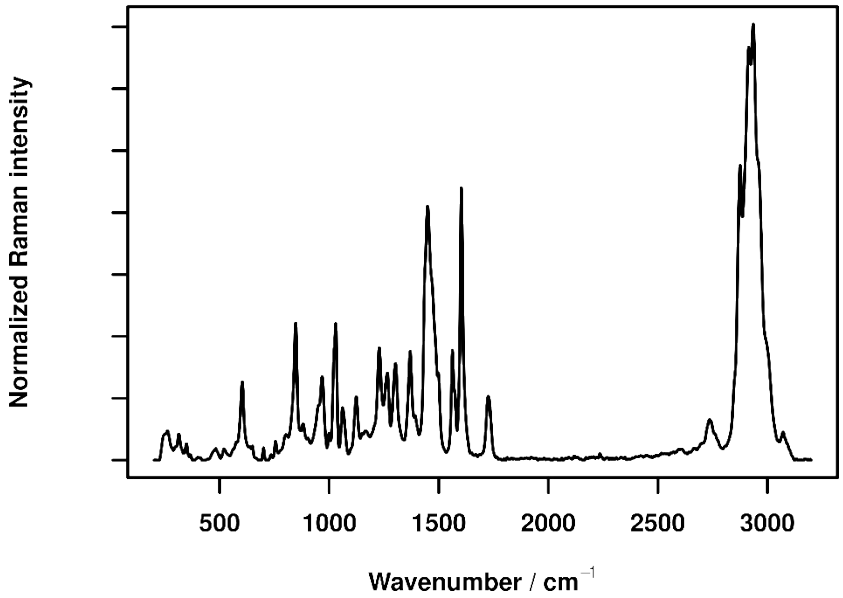

Figure S44. Normalized and background corrected (SNIP, 100 iterations, order 3) FT-Raman spectra of **P2-Zn** between 200 and 3200 cm^{-1}.

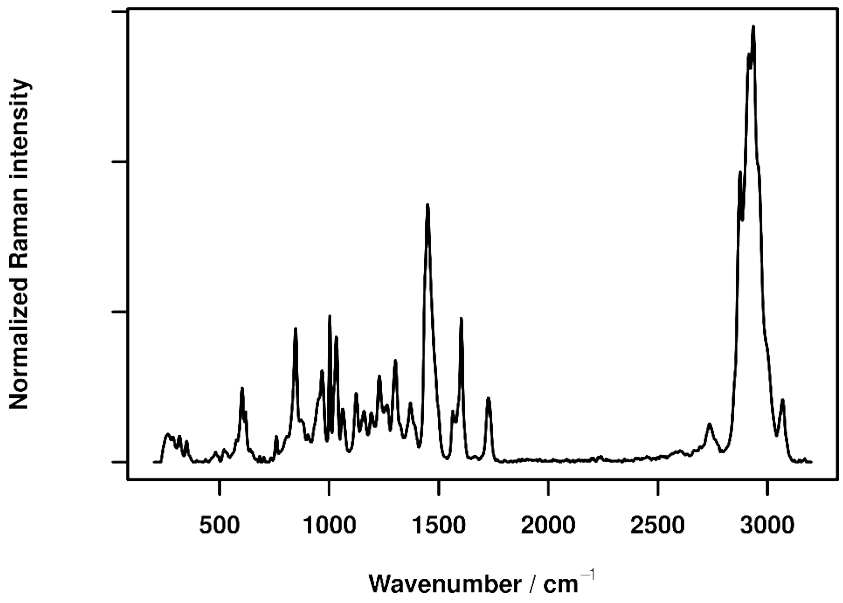

Figure S45. Normalized and background corrected (SNIP, 100 iterations, order 3) FT-Raman spectra of **IPN-1** between 200 and 3200 cm^{-1}.

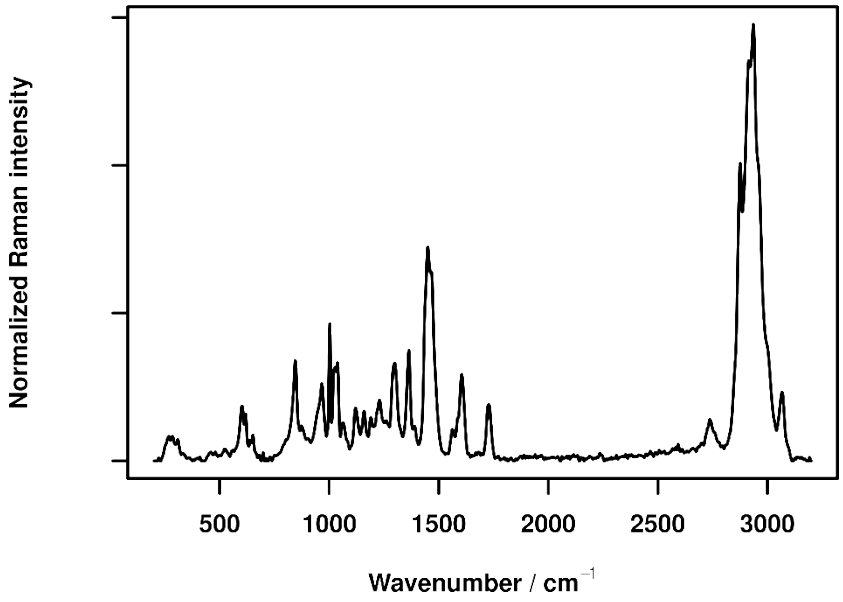

Figure S46. Normalized and background corrected (SNIP, 100 iterations, order 3) FT-Raman spectra of **IPN-2** between 200 and 3200 cm^{-1}.

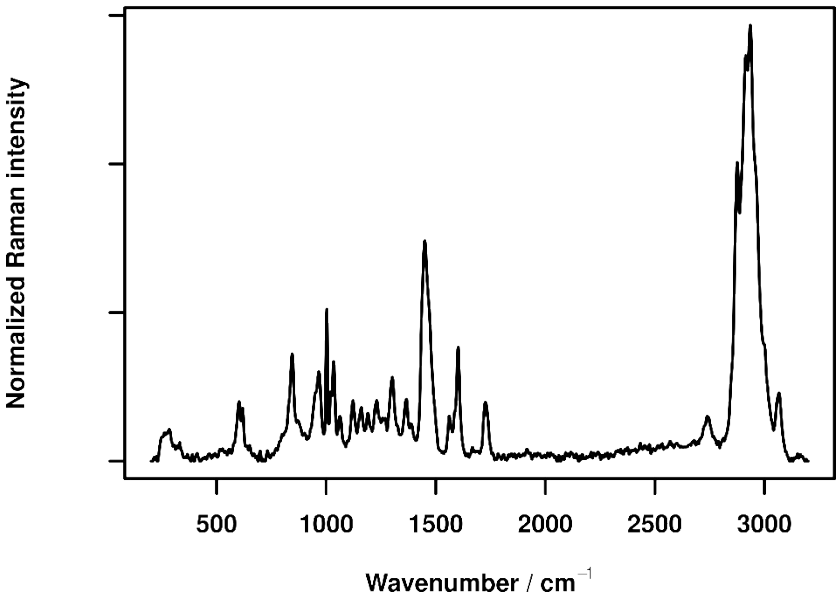

Figure S47. Normalized and background corrected (SNIP, 100 iterations, order 3) FT-Raman spectra of **IPN-3** between 200 and 3200 cm^{-1}.

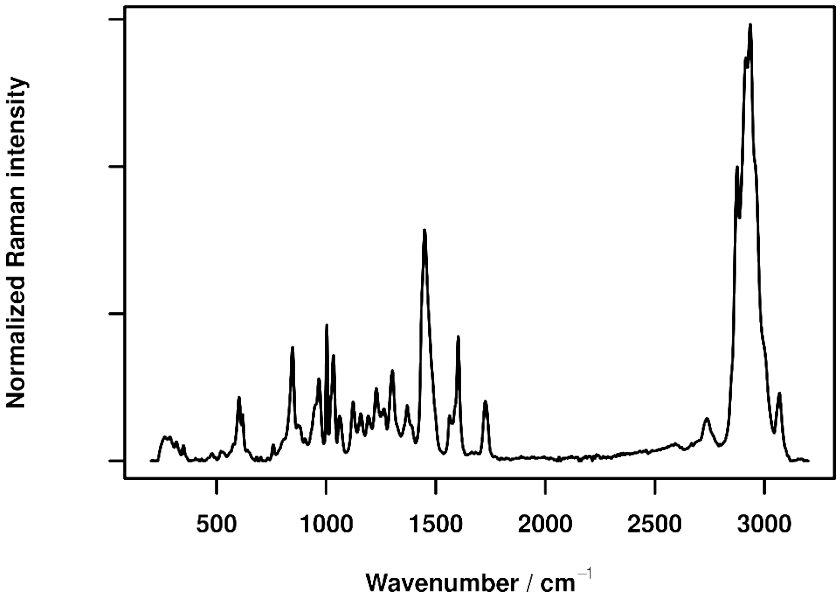

Figure S48. Normalized and background corrected (SNIP, 100 iterations, order 3) FT-Raman spectra of **IPN-4** between 200 and 3200 cm^{-1}.

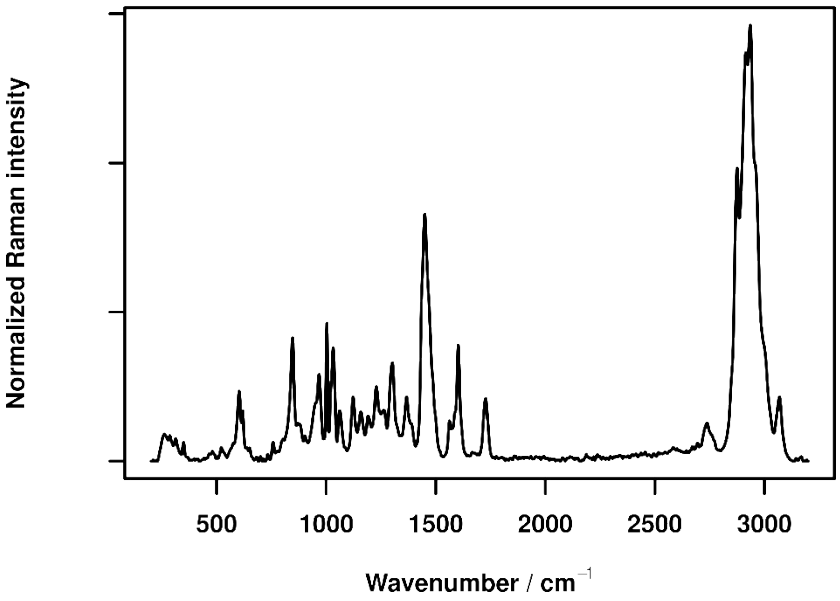

Figure S49. Normalized and background corrected (SNIP, 100 iterations, order 3) FT-Raman spectra of **IPN-5** between 200 and 3200 cm^{-1}.

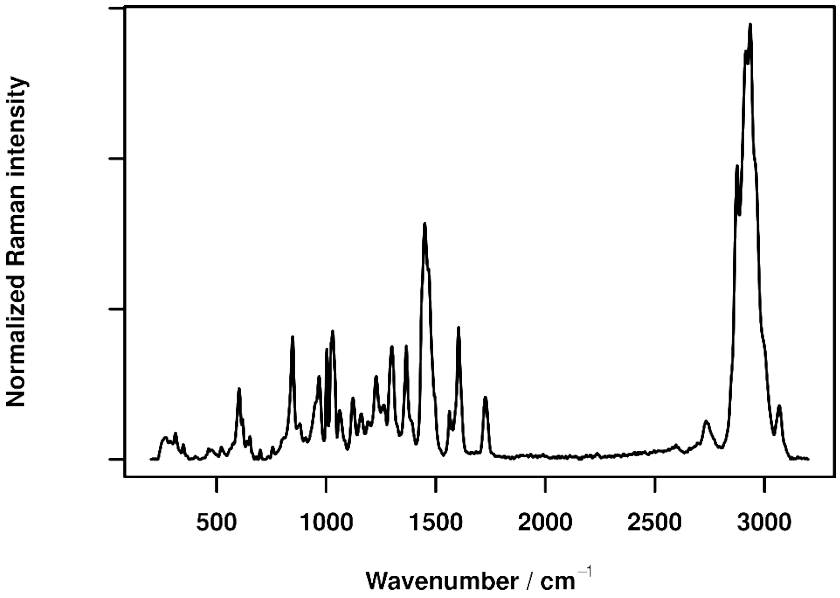

Figure S50. Normalized and background corrected (SNIP, 100 iterations, order 3) FT-Raman spectra of **IPN-6** between 200 and 3200 cm^{-1}.

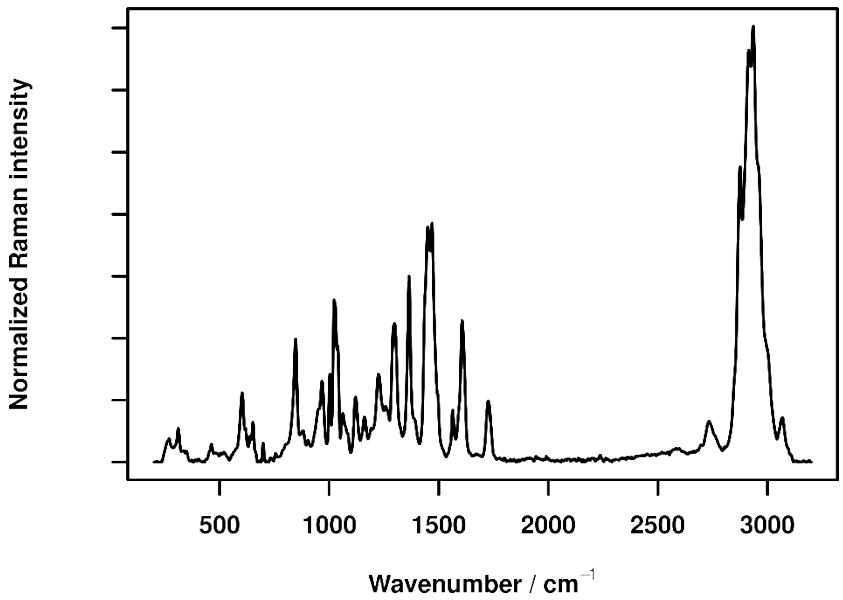

Figure S51. Normalized and background corrected (SNIP, 100 iterations, order 3) FT-Raman spectra of **IPN-7** between 200 and 3200 cm^{-1}.

References

[1] J. Dahlke, J. Kimmig, M. Abend, S. Zechel, J. Vitz, U. S. Schubert and M. D. Hager, *NPG Asia Mater.*, **2020**, *12*, 13.

[2] J. Meurer, J. Hniopek, J. Dahlke, M. Schmitt, J. Popp, S. Zechel and M. D. Hager, *Macromol. Rapid Commun.*, **2021**, *42*, 2000636.

[3] R-Core-Team, Vienna, Austria **2021**, https://www.R-project.org/.

[4] C. G. Ryan, E. Clayton, W. L. Griffin, S. H. Sie, D. R. Cousens, *Nucl. Instrum. Methods Phys. Res*. **1988**, *34*, 396-402.